

Evidence for the Existence of Terminal Scandium Imidos: Mechanistic Studies Involving Imido–Scandium Bond Formation and C–H Activation Reactions

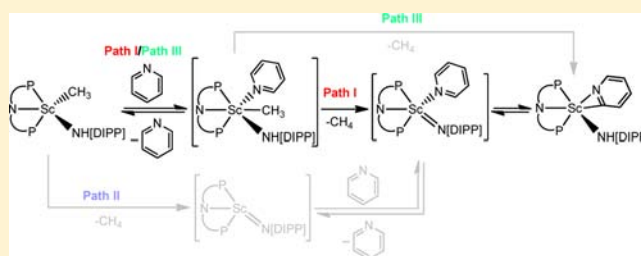
Benjamin F. Wicker, Hongjun Fan,[†] Anne K. Hickey, Marco G. Crestani, Jennifer Scott,[‡] Maren Pink, and Daniel J. Mindiola*

Department of Chemistry, Indiana University, Bloomington, Indiana 47405, United States

Supporting Information

ABSTRACT: The anilide–methyl complex (PNP)Sc(NH[DIPP])(CH₃) (1) [PNP[−] = bis(2-diisopropylphosphino-4-tolyl)amide, DIPP = 2,6-diisopropylphenyl] eliminates methane ($k_{\text{avg}} = 5.13 \times 10^{-4} \text{ M}^{-1}\text{s}^{-1}$ at 50 °C) in the presence of pyridine to generate the transient scandium imido (PNP)Sc=N[DIPP](NC₅H₅) (A-py), which rapidly activates the C–H bond of pyridine in 1,2-addition fashion to form the stable pyridyl complex (PNP)Sc(NH[DIPP])(η^2 -NC₅H₄) (2). Mechanistic studies suggest the C–H activation process to be second order overall: first order in scandium and first order

in substrate (pyridine). Pyridine binding precedes elimination of methane, and α -hydrogen abstraction is overall-rate-determining [the kinetic isotope effect (KIE) for 1-*d*₁ conversion to 2 was 5.37(6) at 35 °C and 4.9(14) at 50 °C] with activation parameters $\Delta H^\ddagger = 17.9(9) \text{ kcal/mol}$ and $\Delta S^\ddagger = -18(3) \text{ cal/(mol K)}$, consistent with an associative-type mechanism. No KIE or exchange with the anilide proton was observed when 1-*d*₃ was treated with pyridine or thermolyzed at 35 or 50 °C. The post-rate-determining step, C–H bond activation of pyridine, revealed a primary KIE of 1.1(2) at 35 °C for the intermolecular C–H activation reaction in pyridine versus pyridine-*d*₅. Complex 2 equilibrated back to the imide A-py slowly, as the isotopomer (PNP)Sc(ND[DIPP])(η^2 -NC₅H₄) (2-*d*₁) converted to (PNP)Sc(NH[DIPP])(η^2 -NC₅H₃D) over 9 days at 60 °C. Molecular orbital analysis of A-py suggested that this species possesses a fairly linear scandium imido motif (169.7°) with a very short Sc–N distance of 1.84 Å. Substituted pyridines can also be activated, with the rates of C–H activation depending on both the steric and electronic properties of the substrate.



1. INTRODUCTION

Imido ligands have become ubiquitous in organometallic chemistry, given that every transition metal triad (with the exception of the groups 9 and 10 triads) has examples of monomeric imido complexes.^{1,2} This ligand class has proven to be very useful: its roles are necessary or have been implicated in many catalytic reactions, including multicomponent coupling processes,^{1,3,4} or simply as a robust ancillary ligand in important catalysts.^{1,d,i,5} Consequently, some of these imido complexes require in-depth studies in order to discern their formation and mode of reactivity.

Our group has explored 3d early transition metal complexes that are both unsaturated and have terminal imido ligands, since we are interested in catalytic transformations involving C–H bond activation and functionalization.^{3,e,f,6} One would anticipate that using more electropositive metal centers such as the group 3 triad would result in even more reactive imido ligands, in view of the polarized nature of the Sc=NR moiety toward a more basic canonical form such as Sc⁺–N[−]R.^{7,8} While complexes of some early transition metals (e.g., Ti) having imido ligands have been well-studied,^{1,d,j} scandium has been resistant to form complexes with such a popular ligand. The first example of a

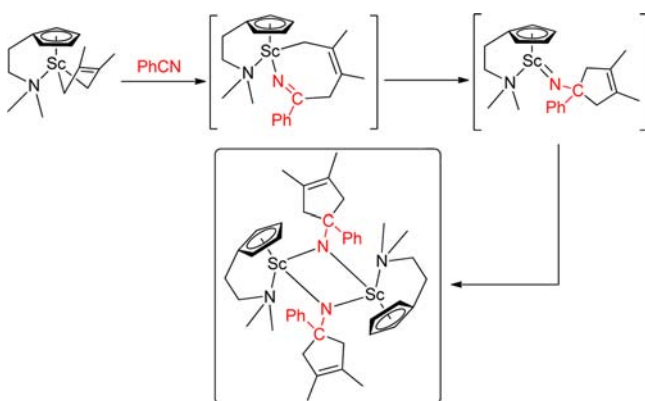
dinuclear scandium imido, which was formed by the insertion of phenyl nitrile into the Sc–C bond of the complex shown in Scheme 1, was reported by Hessen and co-workers.^{9a} They proposed that after the insertion, the alkylimino ring system underwent a cyclization to produce a transient mononuclear scandium imide, which readily dimerized.

While Hessen's system did not engage in C–H activation reactions, presumably because of its dimeric nature, numerous early transition metal imido complexes can intermolecularly activate C–H bonds of alkyl and aryl groups^{3f,10,11} via a 1,2-C–H bond addition mechanism.¹² In general, examples of rare-earth and lanthanide metal ions supported by multiply bonded ligands have seldom been reported,^{2a,3f,7–9,11,13–15} and to our knowledge, an in-depth study into the mechanism of formation and reactivity of these rare species has not been reported, most likely because of their scarcity.¹⁶ One advantage of studying rare-earth or lanthanide complexes containing metal–ligand multiple bonds is that there are many other well-studied transition metal imido systems that are also known to perform

Received: July 24, 2012

Published: October 26, 2012

Scheme 1. Formation of Hessen's Bridging Scandium Imido Complex

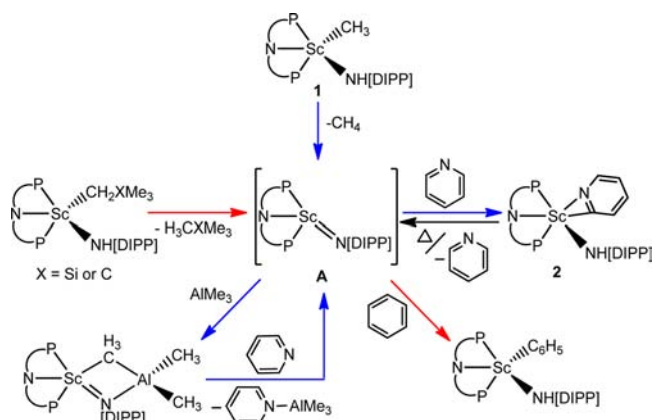


C–H activation and/or catalytic reactions from which we can glean mechanistic insights.¹⁰ While there are many early transition metal imido systems on which one could focus, the most analogous d^0 metal centers that possess ionic radii and Pauling electronegativities comparable to those of Sc(III) (74.5 pm, 1.36) are Zr(IV) (72 pm, 1.33) and Hf(IV) (71 pm, 1.30).¹⁷ For this reason, we focused our attention on Sc(III) imido complexes, as they are rare but comparable to well-known group 4 transition metal imido complexes.

All imido systems that intermolecularly activate C–H bonds are proposed to accomplish this by 1,2 addition of the substrate across the metal imido multiple bond.¹² Bergman and Wolczanski have extensively studied unsaturated imido complexes via kinetic and isotope labeling experiments and established that the C–H activation reaction is zeroth order in substrate, with the formation of the imido as the rate-determining step (RDS).^{10a,b,f–j} Kinetic isotope effect (KIE) experiments showed primary and secondary KIEs for the loss of alkane (α -hydrogen abstraction) to yield the imido intermediate.^{10g,h}

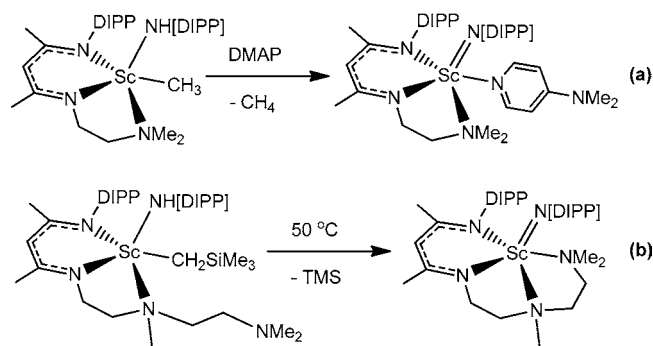
Since our group reported transient titanium alkylidyne (or vanadium alkylidene) complexes using the same PNP ligand¹⁸ that can activate a wide array of hydroaromatic and aliphatic C–H bonds, including those in methane,¹⁹ we wished to extend this work to scandium. We reported a Sc(III) system, (PNP)Sc(NH[DIPP])(CH₃) (**1**) [PNP[−] = bis(2-diisopropylphosphino-4-tolyl)amide, DIPP = 2,6-diisopropylphenyl], that undergoes methane loss in the presence of pyridine to yield the pyridyl complex (PNP)Sc(NH[DIPP])(η^2 -NC₅H₄) (**2**) by virtue of a C–H bond activation process across the transient Sc=N[DIPP] ligand (Scheme 2).^{11,3f} This type of reaction was unprecedented in group 3 and lanthanide metal chemistry.

As shown in Scheme 2, our group first demonstrated that from **1**, the transient imido (PNP)Sc=N[DIPP] (**A**) (or its pyridine adduct **A**-py, which is not shown for the purpose of clarity) can activate the C–H bond of pyridine at the 2-position to yield **2**.^{3f,11} Although the imido intermediate was not isolated, isotopic labeling of the pyridine substrate as well as the isolation of the Al(CH₃)₃-trapped imido zwitterion in the form (PNP)Sc(μ_2 -N[DIPP])(μ_2 -CH₃)[Al(CH₃)₂] supported our assertion that an imido is involved in the C–H activation step.¹¹ Likewise, we showed that an intermediate such as **A** (or an adduct thereof) is most likely responsible for the C–H bond activation of benzene, as (PNP)Sc(NH[DIPP])(CH₂^tBu) and (PNP)Sc(NH[DIPP])(CH₂SiMe₃) form H₃C^tBu or SiMe₄, respectively, and (PNP)Sc(ND[DIPP])(C₆D₅) when dissolved

Scheme 2. Alternate Pathways to the Proposed Scandium Imido Intermediate^a

^aFor clarity, the pyridine adduct of the transient imido (PNP)Sc=N[DIPP] (**A**) is not shown.

in C₆D₆.¹¹ Our proposed intermediate **A**, a terminal scandium imido (or an adduct form that can be prepared by three independent routes) would be soon supported by the isolation of a Sc(III) imido by Chen and co-workers.^{2a,15a–c} Using a tridentate β -diketiminato ligand, they were able to generate the imido by α -hydrogen abstraction (Scheme 3a), which was most

Scheme 3. Generation of Chen's Sc(III) Imidos via α -Hydrogen Abstraction with the Aid of (a) DMAP or (b) a Pendant Amine Group

likely promoted by using 4-*N,N*-dimethylaminopyridine (DMAP) as a Lewis base. Chen and co-workers also prepared a DMAP-free scandium imido by using a pendant dimethylamino group (Scheme 3b).^{15b} To the best of our knowledge, the latter system is surprisingly inert toward intermolecular C–H bonds with high pK_a 's,^{15c} presumably because of the congested environment about the Sc(III) ion. Very recently, Cui and co-workers observed intramolecular C–H bond activation of a pendant arene by a scandium imido complex.^{15d} In the latter case, a Lewis base such as DMAP was also necessary to promote formation of the imido ligand.

In this paper, we present convincing synthetic and mechanistic evidence for the formation of a transient mononuclear Sc(III) imido. Along with isotopic labeling and KIE studies, we also extracted thermodynamic parameters for the formation of the pyridyl complex via a transient imido adduct, which was also corroborated by theoretical studies. We investigated the role of pyridine in the C–H activation reaction pathway by analyzing competing mechanistic scenarios

(whether methane loss occurs before or after pyridine binding) as well as the effect of substituted pyridines on the rate of the reaction, including some showcase reactivity. Our study represents the first detailed investigation of metal imido formation and C–H bond reactivity for any rare-earth or lanthanide system.

2. EXPERIMENTAL SECTION

General Considerations. Unless otherwise stated, all operations were performed in an M. Braun Lab Master double drybox under an atmosphere of purified nitrogen or using standard high-vacuum Schlenk techniques under an argon atmosphere.²⁰ Anhydrous *n*-pentane, *n*-hexane, and toluene were purchased from Aldrich in Sure-Sealed reservoirs (18 L) and dried by passage through a column of activated alumina and then a Q-5 column.²¹ 1,4-Dioxane was dried by stirring in small pieces of Na metal for 24 h, followed by filtration through activated alumina. C₆D₆ (purchased from Cambridge Isotope Laboratories) was degassed and dried over 4 Å molecular sieves for at least 24 h before use. Celite, alumina, and 4 Å molecular sieves were activated under vacuum overnight at 200 °C. (PNP)ScCl₂,¹¹ (PNP)Sc(CH₃)(Br),¹¹ and complexes **1**,¹¹ **2**,¹¹ **8**,^{3f} and **9**^{3f} were synthesized according to literature protocols. DMAP was purchased from Aldrich and cycled into the box under vacuum. 2-Picoline, 4-picoline, and 2-fluoropyridine were vacuum-distilled from CaH₂ and stored in the drybox over 4 Å molecular sieves. LiND[DIPP] and LiNH[DIPP] were prepared by addition of equimolar amounts of 2.5 M ⁿ-BuLi in *n*-hexane to D₂N[DIPP] and H₂N[DIPP], respectively, in *n*-hexane. The suspensions were stirred overnight and then filtered, and the solids were washed with hexanes and dried under vacuum. D₂N[DIPP] and H₂N[DIPP] were dried over CaH₂ and distilled before being brought into the glovebox; both were passed through alumina and stored over 4 Å molecular sieves. The complex (PNP)Sc(ND[DIPP])(Cl) was prepared analogously to its isotopologue (PNP)Sc(NH[DIPP])(Cl).¹¹ ¹H, ¹³C, and ³¹P NMR spectra were recorded on Varian 400 and 300 MHz NMR spectrometers. ¹H and ¹³C NMR spectral data are reported with reference to solvent resonances (residual C₆D₅H in C₆D₆, 7.16 and 128.0 ppm, respectively), and ³¹P NMR chemical shifts are reported with respect to external H₃PO₄ (aqueous solution, 0.0 ppm). Multinuclear NMR spectral data for all complexes are included in the Supporting Information (SI).²² Repeated attempts to obtain satisfactory microanalysis of the compounds failed because of their extreme sensitivity to air and moisture and quite possibly their incomplete combustion. We have therefore provided high-resolution 1D and 2D NMR spectra as proof of their purity and in lieu of combustion elemental analysis data. Melting points for selected compounds were measured in flame-sealed capillaries on an Electrothermal Mel Temp apparatus. IR spectra were measured using a Thermo Scientific Nicolet 6700 spectrometer. Samples were prepared by crushing and mixing the compounds with KBr (FT-IR grade, ≥99% trace metals basis, Sigma-Aldrich) and pressing the mixture into a pellet. All of the IR spectral data are included in the SI.

Syntheses. (CH₃)₂C=N[DIPP]. A round-bottom flask was charged with 6.0 mL (5.64 g, 31.8 mmol) of H₂N[DIPP], 20.0 mL (17.0 g, 163.2 mmol) of 2,2-dimethoxypropane, and 155 mg (1.6 mmol) of sulfuric acid in 200 mL of ethanol. The solution was refluxed for 12 h under nitrogen and then cooled. The volatiles were removed via rotary evaporator, yielding the product as a brown oil (6.2 g, 28.6 mmol, 90% yield). The ¹H and ¹³C NMR spectra were consistent with those from a previously reported synthesis of (CH₃)₂C=N[DIPP].²³

D₂N[DIPP]. A round-bottom flask was charged with (CH₃)₂C=N[DIPP] (6.2 g, 28.6 mmol), 75.0 mL (83.03 g, 4145.0 mmol) of D₂O, and 1 mL of 3.0 M CF₃CO₂D in D₂O [prepared by adding 5.29 mL of (CF₃C=O)₂O to 25 mL of D₂O]. The oil remained immiscible with the D₂O while the reaction mixture was refluxed for 6 h under nitrogen. After the mixture was cooled, the product was extracted into *n*-hexane, dried with Mg₂SO₄, and filtered through Celite. The volatiles in the filtrate were removed by a rotary evaporator, yielding a yellow oil (4.7 g, 26.3 mmol, 92% yield). The oil was further purified by

drying over CaH₂ and distilled under reduced pressure at 120 °C with a short-path distillation apparatus. Room-temperature water was used in the distillation column, and the receiving flask was immersed in a –78 °C bath. The oil was degassed, taken into the glovebox, and used for subsequent reactivity.

(PNP)Sc(CD₃)(I). A solution of CD₃MgI (0.69 mL, 1.0 M) in diethyl ether was added dropwise to a stirring suspension of (PNP)ScCl₂ (376.0 mg, 0.69 mmol) in toluene (15 mL) at –35 °C. The reaction mixture was stirred for 5 h, after which 1 mL of anhydrous 1,4-dioxane was added to promote the precipitation of magnesium salts. The resulting cloudy, yellow suspension was filtered through Celite, and the filtrate was concentrated to <1 mL and placed in the freezer overnight. Yellow crystals of (PNP)Sc(CD₃)(I) were isolated upon standing at –35 °C overnight (256 mg, 0.36 mmol, 61% yield). The NMR spectroscopic data were similar to those for the previously reported complex (PNP)Sc(CH₃)(Br),¹¹ except for the absence of the methyl resonance. Mp: 230–240 °C (decomp). ¹H NMR (25 °C, 399.93 MHz, C₆D₆): δ 7.24 (s, 1H, C₆H₃), 7.02 (br, 1H, C₆H₃), 6.90–6.72 (m, 4H, C₆H₃), 2.14 (s, 3H, C₆H₃–CH₃), 2.10 (s, 3H, C₆H₃–CH₃), 2.09–1.94 (m, 3H, CHMe₂), 1.89 (sept, ³J_{H–H} = 6.8 Hz, 1H, CHMe₂), 1.40–1.00 (m, 18H, PCH(CH₃)₂), 0.85 (m, 6H, PCH(CH₃)₂). ¹³C NMR (25 °C, 100.57 MHz, C₆D₆): δ 160.6 (d, C₆H₃), 159.2 (d, C₆H₃), 133.8 (s, C₆H₃), 133.7 (s, C₆H₃), 133.6 (s, C₆H₃), 133.5 (s, C₆H₃), 127.73 (s, C₆H₃), 129.69 (s, C₆H₃), 121.5 (s, C₆H₃), 121.4 (s, C₆H₃), 118.4 (s, C₆H₃), 118.3 (s, C₆H₃), 24.5 (t, PCH(CH₃)₂), 21.1 (d, PCH(CH₃)₂), 20.1–18.6 (m, PCH(CH₃)₂/PCH(CH₃)₂), 16.9 (d, PCH(CH₃)₂). ³¹P NMR (25 °C, 161.98 MHz, C₆D₆): δ 3.16 and 2.37 (br, overlapping singlets, Δν_{1/2} = 253 Hz).

(PNP)Sc(ND[DIPP])(CH₃) (1-*d*₁). A solution of LiND[DIPP] (153.9 mg, 0.83 mmol) in *n*-hexane (3 mL), with a few drops of ether added to solubilize the salt, was added dropwise to a stirring suspension of (PNP)Sc(CH₃)(Br) (475 mg, 0.83 mmol) in *n*-hexane (15 mL). The reaction mixture was stirred for 5 h. The resulting cloudy, yellow suspension was filtered through Celite, and the filtrate was concentrated to 5 mL and placed in the freezer overnight. Yellow crystals of 1-*d*₁ were isolated upon standing at –35 °C overnight (258.1 mg, 0.40 mmol, 48% yield). The NMR spectra obtained for 1-*d*₁ were identical to those reported for **1**, except for the notable absence of the anilide proton resonance at 6.01 ppm in the ¹H NMR spectrum.

(PNP)Sc(NH[DIPP])(CD₃) (1-*d*₃). A solution of LiNH[DIPP] (30.9 mg, 0.17 mmol) in *n*-hexane (3 mL), with a few drops of ether added to solubilize the salt, was added dropwise to a stirring suspension of (PNP)Sc(CD₃)(I) (104.5 mg, 0.17 mmol) in *n*-hexane (15 mL). The reaction mixture was stirred for 5 h. The resulting cloudy, yellow suspension was filtered through Celite, and the filtrate was concentrated to <1 mL and placed in the freezer overnight. Yellow crystals of 1-*d*₃ were isolated upon standing at –35 °C overnight (45 mg, 0.07 mmol, 40% yield). Mp: 138–142 °C. The NMR spectra obtained for 1-*d*₃ were identical to those reported for **1**, except for the notable absence of the scandium methyl resonance at 0.29 ppm in the ¹H NMR spectrum. IR (KBr): ν_{NH} 3312 cm^{–1}.

(PNP)Sc(ND[DIPP])(CD₃) (1-*d*₄). A solution of CD₃MgI (1.0 M, 0.68 mL) dissolved in dioxane (1 mL) was added to a solution of (PNP)Sc(ND[DIPP])(Cl) (234.3 mg, 0.34 mmol) dissolved in toluene (10 mL). The reaction mixture was stirred for 2 h and then filtered through a pad of Celite, after which the filtrate was concentrated to 1 mL. Crystals of 1-*d*₄ were isolated upon standing at –35 °C overnight (90.5 mg, 0.14 mmol, 40% yield). The NMR spectra obtained for 1-*d*₄ were identical to those reported for **1**, except for the notable absences of the anilide proton resonance at 6.01 ppm and the scandium methyl resonance at 0.29 ppm in the ¹H NMR spectrum.

(PNP)Sc(ND[DIPP])(*η*²-NC₅H₄) (2-*d*₁). In a vial, a solution of 2-bromopyridine (39.1 mg, 0.25 mmol) in tetrahydrofuran (THF) (3 mL) was cooled to –100 °C (dry ice/ethanol bath), and to this cold solution was added 0.1 mL of 2.5 M *n*-BuLi in *n*-hexane. The solution was stirred for 10 min and then added dropwise cold to a stirring suspension of (PNP)Sc(ND[DIPP])(Cl) (171.0 mg, 0.25 mmol) in THF (15 mL) at –100 °C. The reaction mixture was stirred for 1 h,

after which the THF was evaporated under vacuum. The residue was extracted into *n*-pentane, and the resulting cloudy, yellow suspension was filtered through Celite. The filtrate was concentrated to <1 mL and allowed to stand at $-35\text{ }^{\circ}\text{C}$ overnight, after which yellow crystals of 2-*d*₁ were isolated (88.8 mg, 0.12 mmol, 49.3% yield). The ratio of 2-*d*₁ to protonated anilide was 3:1. ^1H NMR (25 $^{\circ}\text{C}$, 399.93 MHz, C_6D_6): δ 8.33 (d, $^3J_{\text{H-H}} = 5.2$ Hz, 1H, 6-H in NC_5H_4), 7.88 (d, $^3J_{\text{H-H}} = 7.3$ Hz, 1H, 3-H in NC_5H_4), 7.28 (dd, $^3J_{\text{H-H}} = 8.3$, 4.5 Hz, 1H, C_6H_3), 7.23–7.16 (m, 3H, C_6H_3), 7.09 (td, $^3J_{\text{H-H}} = 7.4$, 1.0 Hz, 1H, NC_5H_4), 6.91 (d, $^3J_{\text{H-H}} = 7.6$ Hz, 2H, C_6H_3), 6.89–6.83 (m, 3H, C_6H_3), 6.67 (ddd, $^3J_{\text{H-H}} = 6.0$, 5.3, 1.0 Hz, 1H, NC_5H_4), 6.18 (s, 1H, NH), 3.37 (br s, 2H, Ar– CHMe_2), 2.22 (s, 3H, $\text{C}_6\text{H}_3\text{--CH}_3$), 2.16 (s, 3H, $\text{C}_6\text{H}_3\text{--CH}_3$), 2.06–1.82 (m, 3H, PCHMe_2), 1.65 (m, 1H, PCHMe_2), 1.35 (d, $^3J_{\text{H-H}} = 6.4$ Hz, 12H, Ar– $\text{CH}(\text{CH}_3)_2$), 1.26–1.12 (m, 6H, $\text{PCH}(\text{CH}_3)_2$), 1.06–0.80 (m, 12H, $\text{PCH}(\text{CH}_3)_2$), 0.74–0.66 (m, 3H, $\text{PCH}(\text{CH}_3)_2$), 0.46–0.36 (m, 3H, $\text{PCH}(\text{CH}_3)_2$). ^{13}C NMR (23 $^{\circ}\text{C}$, 100.6 MHz, C_6D_6): δ 217.2 (s, Sc–C, $\eta^2\text{-NC}_5\text{H}_4$), 161.1 (d, C_6H_3), 160.4 (d, C_6H_3), 151.5 (s, C_6H_3), 145.7 (s, C_6H_3), 134.0 (s, NC_5H_4), 132.9 (s, C_6H_3), 132.8 (s, C_6H_3), 132.6 (s, C_6H_3), 132.4 (s, C_6H_3), 130.2 (s, NC_5H_4), 128.1 (s, C_6H_3), 127.8 (s, C_6H_3), 126.1 (d, C_6H_3), 122.7 (s, NC_5H_4), 121.9 (s, NC_5H_4), 120.5 (d, C_6H_3), 119.7 (s, C_6H_3), 119.5 (s, C_6H_3), 119.4 (s, C_6H_3), 119.2 (s, C_6H_3), 118.3 (d, C_6H_3), 116.0 (s, C_6H_3), 28.8 (s, Ar– CHMe_2), 25.2 (d, PCHMe_2), 24.3 (s, Ar– $\text{CH}(\text{CH}_3)_2$), 23.9 (s, Ar– $\text{CH}(\text{CH}_3)_2$), 23.5 (d, PCHMe_2), 20.8 (s, $\text{C}_6\text{H}_3\text{--CH}_3$), 20.7 (s, $\text{C}_6\text{H}_3\text{--CH}_3$), 20.1 (d, PCHMe_2), 19.9 (d, PCHMe_2), 19.5 (d, Ar– CHMe_2), 19.5 (s, $\text{PCH}(\text{CH}_3)_2$), 19.4 (d, $\text{PCH}(\text{CH}_3)_2$), 19.1 (s, $\text{PCH}(\text{CH}_3)_2$), 19.0 (s, $\text{PCH}(\text{CH}_3)_2$), 18.8 (d, $\text{PCH}(\text{CH}_3)_2$), 18.75 (d, $\text{PCH}(\text{CH}_3)_2$), 17.8 (s, $\text{PCH}(\text{CH}_3)_2$), 16.5 (s, $\text{PCH}(\text{CH}_3)_2$). ^{31}P NMR (23 $^{\circ}\text{C}$, 121.5 MHz, C_6D_6): δ 5.1 (br, $\Delta\nu_{1/2} = 131$ Hz), 4.5 (br, $\Delta\nu_{1/2} = 131$ Hz).

(PNP)Sc(NH[DIPPI])($\eta^2\text{-NC}_5\text{H}_3\text{-4-N}(\text{CH}_3)_2$) (3). A J-Young tube was charged with 1 (54.3 mg, 0.082 mmol). To this was added a solution of DMAP (10.0 mg, 0.082 mmol) in C_6D_6 (1.5 mL). The reaction quickly changed color from yellow to orange. The mixture was heated at 65 $^{\circ}\text{C}$ for 30 min, and the solvent was removed under reduced pressure. The residue was extracted with 1 mL of toluene and filtered through a pad of Celite. The Celite was then washed with 1 mL of *n*-hexane. From the filtrate, yellow crystals of 3 were isolated upon standing at $-35\text{ }^{\circ}\text{C}$ overnight (34.1 mg, 0.044 mmol, 55.4% yield). Mp: 126–164 $^{\circ}\text{C}$ (decomp). ^1H NMR (25 $^{\circ}\text{C}$, 300.1 MHz, C_6D_6): δ 8.20 (d, $^3J_{\text{H-H}} = 6.1$ Hz, 1H, NC_5H_3), 7.31 (dd, $^3J_{\text{H-H}} = 8.3$, 4.5 Hz, 1H, C_6H_3), 7.25 (dd, $^3J_{\text{H-H}} = 8.7$, 4.4 Hz, 1H, C_6H_3), 7.21 (d, $^3J_{\text{H-H}} = 7.6$ Hz, 2H, C_6H_3), 7.18 (d, $^3J_{\text{H-H}} = 2.3$ Hz, NC_5H_3), 7.01–6.90 (m, 4H, C_6H_3), 6.78 (t, $^3J_{\text{H-H}} = 7.5$ Hz, 1H, C_6H_3), 6.15 (dd, $^3J_{\text{H-H}} = 6.2$, 2.7 Hz, 1H, NC_5H_3), 6.08 (s, 1H, NH), 3.50 (br, 2H, $\text{CH}(\text{CH}_3)_2$), 2.37 (s, 6H, $\text{N}(\text{CH}_3)_2$), 2.24 (s, 3H, $\text{C}_6\text{H}_3\text{--CH}_3$), 2.18 (s, 3H, $\text{C}_6\text{H}_3\text{--CH}_3$), 2.14–1.89 (m, 3H, $\text{PCH}(\text{CH}_3)_2$), 1.83 (sept, $^3J_{\text{H-H}} = 6.8$ Hz, 1H, $\text{PCH}(\text{CH}_3)_2$), 1.42 (d, $^3J_{\text{H-H}} = 6.8$ Hz, 6H, $\text{CH}(\text{CH}_3)_2$), 1.39 (d, $^3J_{\text{H-H}} = 6.7$ Hz, 6H, $\text{CH}(\text{CH}_3)_2$), 1.31 (dd, $^3J_{\text{H-H}} = 14.7$, 7.0 Hz, 3H, $\text{PCH}(\text{CH}_3)_2$), 1.26 (dd, $^3J_{\text{H-H}} = 14.2$, 7.0 Hz, $\text{PCH}(\text{CH}_3)_2$), 1.11–1.02 (m, 6H, $\text{PCH}(\text{CH}_3)_2$), 0.98–0.89 (m, 6H, $\text{PCH}(\text{CH}_3)_2$), 0.83 (dd, $^3J_{\text{H-H}} = 15.3$, 6.8 Hz, 3H, $\text{PCH}(\text{CH}_3)_2$), 0.67 (dd, $^3J_{\text{H-H}} = 14.6$, 7.0 Hz, 3H, $\text{PCH}(\text{CH}_3)_2$). $^{13}\text{C}\{^1\text{H}\}$ NMR (25 $^{\circ}\text{C}$, 100.6 MHz, C_6D_6): δ 213.8 (br, Sc–C, $\eta^2\text{-NC}_5\text{H}_3$), 161.4 (d, C_6H_3), 161.0 (d, C_6H_3), 152.1 (s, C_6H_3), 151.9 (s, C_6H_3), 144.6 (s, NC_5H_3), 134.1 (br, C_6H_3), 132.9 (s, NC_5H_3), 132.6 (s, C_6H_3), 132.5 (s, C_6H_3), 132.4 (C_6H_3), 127.3 (d, C_6H_3), 125.7 (d, C_6H_3), 122.7 (s, C_6H_3), 120.5 (d, C_6H_3), 119.9 (d, C_6H_3), 119.7 (d, C_6H_3), 118.4 (d, C_6H_3), 115.6 (s, NC_5H_3), 111.2 (s, NC_5H_3), 106.8 (s, NC_5H_3), 38.6 ($\text{N}(\text{CH}_3)_2$), 28.7 (br, anilide $\text{CH}(\text{CH}_3)_2$), 25.3 (d, $\text{CH}(\text{CH}_3)_2$), 24.6 (s, $\text{CH}(\text{CH}_3)_2$), 24.1 (s, Ar– CH_3), 23.7 (d, $\text{CH}(\text{CH}_3)_2$), 20.9 (d, $\text{CH}(\text{CH}_3)_2$), 20.4 (d, $\text{CH}(\text{CH}_3)_2$), 20.1 (d, $\text{CH}(\text{CH}_3)_2$), 19.9–19.2 (m, $\text{CH}(\text{CH}_3)_2/\text{CH}(\text{CH}_3)_2$), 18.0 (s, $\text{CH}(\text{CH}_3)_2$), 16.7 (d, $\text{CH}(\text{CH}_3)_2$). $^{31}\text{P}\{^1\text{H}\}$ NMR (25 $^{\circ}\text{C}$, 162.0 MHz, C_6D_6): δ 4.7 ($\Delta\nu_{1/2} = 84.0$ Hz), 3.8 ($\Delta\nu_{1/2} = 66.0$ Hz). IR (KBr): ν_{NH} 3309 cm^{-1} .

(PNP)Sc(NH[DIPPI])($\eta^2\text{-NC}_5\text{H}_3\text{-4-CH}_3$) (4). 1 (48.5 mg, 0.073 mmol) was placed in a J-Young tube and dissolved in C_6D_6 . To this was added 2 drops of 4-picoline. The mixture was heated at 65 $^{\circ}\text{C}$ for 12 h, and the solvent and excess 4-picoline were removed under reduced pressure. The residue was extracted into hexanes (3 mL) and filtered.

From the filtrate, yellow crystals of 4 were isolated upon standing at $-35\text{ }^{\circ}\text{C}$ overnight (35.5 mg, 0.048 mmol, 68.5% yield). Mp: 146–170 $^{\circ}\text{C}$ (decomp). ^1H NMR (25 $^{\circ}\text{C}$, 300.1 MHz, C_6D_6): δ 8.28 (d, $^3J_{\text{H-H}} = 5.3$ Hz, 1H, NC_5H_3), 7.81 (s, 1H, NC_5H_3), 7.28 (dd, $^3J_{\text{H-H}} = 8.3$, 4.4 Hz, 1H, C_6H_3), 7.25–7.17 (m, 3H, C_6H_3), 7.02–6.82 (m, 5H, C_6H_3), 6.59 (d, $^3J_{\text{H-H}} = 5.2$ Hz, 1H, NC_5H_3), 6.16 (s, 1H, NH), 3.39 (br, 2H, $\text{CH}(\text{CH}_3)_2$), 2.23 (s, 3H, $\text{C}_6\text{H}_3\text{--CH}_3$), 2.18 (s, 3H, $\text{C}_6\text{H}_3\text{--CH}_3$), 1.94 (s, 3H, $\text{NC}_5\text{H}_3\text{--CH}_3$), 2.09–1.84 (m, 3H, $\text{PCH}(\text{CH}_3)_2$), 1.72 (sept, $^3J_{\text{H-H}} = 7.0$ Hz, 1H, $\text{PCH}(\text{CH}_3)_2$), 1.36 (pseudo t, $^3J_{\text{H-H}} = 6.4$ Hz, 12H, $\text{CH}(\text{CH}_3)_2$), 1.27–1.15 (m, 6H, $\text{PCH}(\text{CH}_3)_2$), 1.09–0.95 (m, 6H, $\text{PCH}(\text{CH}_3)_2$), 0.94–0.84 (m, 6H, $\text{PCH}(\text{CH}_3)_2$), 0.76 (dd, $^3J_{\text{H-H}} = 15.3$, 6.8 Hz, 3H, $\text{PCH}(\text{CH}_3)_2$), 0.50 (dd, $^3J_{\text{H-H}} = 14.6$, 7.0 Hz, 3H, $\text{PCH}(\text{CH}_3)_2$). $^{13}\text{C}\{^1\text{H}\}$ NMR (25 $^{\circ}\text{C}$, 75.5 MHz, C_6D_6): δ 216.0 (br, Sc–C, $\eta^2\text{-NC}_5\text{H}_3$), 161.1 (d, C_6H_3), 160.6 (d, C_6H_3), 151.6 (s, C_6H_3), 145.1 (s, C_6H_3), 143.7 (s, NC_5H_3), 134.1 (br, C_6H_3), 132.8 (s, NC_5H_3), 132.7 (s, C_6H_3), 132.4 (s, C_6H_3), 131.0 (s, C_6H_3), 126.1 (d, C_6H_3), 123.4 (s, NC_5H_3), 122.7 (s, C_6H_3), 120.5 (d, C_6H_3), 119.8 (d, C_6H_3), 119.5 (d, C_6H_3), 118.5 (d, C_6H_3), 115.9 (s, NC_5H_3), 28.9 (br, anilide $\text{CH}(\text{CH}_3)_2$), 25.3 (d, $\text{CH}(\text{CH}_3)_2$), 24.4 (s, Ar– CH_3), 24.0 (s, Ar– CH_3), 23.6 (d, $\text{CH}(\text{CH}_3)_2$), 20.9 (d, $\text{CH}(\text{CH}_3)_2$), 20.6 ($\text{NC}_5\text{H}_3\text{--CH}_3$), 20.4–18.7 (m, $\text{CH}(\text{CH}_3)_2/\text{CH}(\text{CH}_3)_2/\text{anilide } \text{CH}(\text{CH}_3)_2$), 17.9 (s, $\text{CH}(\text{CH}_3)_2$), 16.6 (d, $\text{CH}(\text{CH}_3)_2$). $^{31}\text{P}\{^1\text{H}\}$ NMR (25 $^{\circ}\text{C}$, 162.0 MHz, C_6D_6): δ 4.7 ($\Delta\nu_{1/2} = 86.6$ Hz), 3.9 ($\Delta\nu_{1/2} = 84.5$ Hz). IR (KBr): ν_{NH} 3311 cm^{-1} .

(PNP)Sc(NH[DIPPI])($\eta^2\text{-NC}_5\text{H}_3\text{-2-CH}_3$) (5) and (PNP)Sc(NH[DIPPI])($\kappa^2\text{-C,N-NC}_5\text{H}_4\text{-2-CH}_2$) (6). 1 (40.3 mg, 0.061 mmol) was placed in a J-Young tube and dissolved in C_6D_6 . To this was added 2 drops of 2-picoline. The mixture was heated at 65 $^{\circ}\text{C}$ for 12 h, and the solvent and excess 2-picoline removed under reduced pressure. The residue was extracted into *n*-hexane (3 mL) and filtered through a small pad of Celite. From the filtrate, yellow crystals of a mixture of 5 and 6 were isolated upon standing at $-35\text{ }^{\circ}\text{C}$ overnight (24.1 mg, 0.032 mmol, 53.9% yield). Mp: 118–202 $^{\circ}\text{C}$ (decomp). For the 5/6 mixture: ^1H NMR (25 $^{\circ}\text{C}$, 399.93 MHz, C_6D_6): δ 7.75 (d, 7.1 Hz), 7.38 (dd, $J_{\text{H-H}} = 8.3$, 4.1 Hz), 7.29–7.13 (m), 7.13–7.03 (m), 7.02–6.83 (m), 6.74 (td, $J_{\text{H-H}} = 7.6$, 1.5 Hz), 6.62–6.51 (m), 6.17 (s, N–H), 6.08 (s, N–H), 5.85 (t, $J_{\text{H-H}} = 6.1$ Hz), 3.47 (br), 3.20 (br), 2.65 (sept, 6.6 Hz), 2.45 (s), 2.24 (s), 2.23 (s), 2.20 (s), 2.19 (s), 2.17–1.78 (m), 1.99 (s), 1.66 (sept, $J_{\text{H-H}} = 7.1$ Hz), 1.45 (d, 6.6 Hz), 1.40 (d, 6.6 Hz), 1.37–0.5 (m), 0.22 (dd, $J_{\text{H-H}} = 14.7$, 7.0 Hz). ^{13}C NMR (25 $^{\circ}\text{C}$, 100.57 MHz, C_6D_6): δ 216.9 (br, Sc–C, $\eta^2\text{-NC}_5\text{H}_3$), 146.8 (s, NC_6H_3), 133.7 (s, NC_6H_3), 133.2 (s, C_6H_3), 132.4 (s, C_6H_3), 132.2 (s, C_6H_3), 132.15 (s, C_6H_3), 132.0 (s, C_6H_3), 131.8 (s, C_6H_3), 130.1 (s, NC_6H_3), 127.9 (s, NC_6H_3), 126.0 (s, C_6H_3), 122.6 (s, C_6H_3), 122.4 (s, C_6H_3), 121.8 (s, NC_6H_3), 119.9 (d, C_6H_3), 119.3 (s, NC_6H_3), 117.9 (d, C_6H_3), 117.7 (d, C_6H_3), 116.8 (s, NC_6H_3), 116.3 (s, NC_6H_3), 115.6 (s, NC_6H_3), 110.4 (s, NC_6H_3), 53.2 (s, Sc– $\text{CH}_2\text{--NC}_5\text{H}_4$), 28.9 (s, $\text{NC}_5\text{H}_3\text{--CH}_3$), 25.5 (d, $\text{PCH}(\text{CH}_3)_2$), 25.0 (s, $\text{PCH}(\text{CH}_3)_2$), 23.9 (s, $\text{PCH}(\text{CH}_3)_2$), 23.8 (s, $\text{PCH}(\text{CH}_3)_2$), 23.2 (s, $\text{PCH}(\text{CH}_3)_2$), 22.3 (s, $\text{PCH}(\text{CH}_3)_2$), 20.5 (Ar– CH_3), 20.1 (s, $\text{PCH}(\text{CH}_3)_2$), 17.2 (s, $\text{PCH}(\text{CH}_3)_2$). $^{31}\text{P}\{^1\text{H}\}$ NMR (25 $^{\circ}\text{C}$, 161.98 MHz, C_6D_6): δ 5.58 ($\Delta\nu_{1/2} = 118$ Hz), 4.83 ($\Delta\nu_{1/2} = 132$ Hz). IR (KBr): ν_{NH} 3313 cm^{-1} .

(PNP)Sc(NH[DIPPI])($\kappa^2\text{-C,N-NC}_5\text{H}_3\text{-2-CH}_2\text{-6-CH}_3$) (7). 1 (36.3 mg, 0.055 mmol) was placed in a J-Young tube and dissolved in C_6D_6 . To this was added 2 drops of 2,6-lutidine. The mixture was heated at 65 $^{\circ}\text{C}$ for 12 h, and the solvent and excess 2,6-lutidine were removed under reduced pressure. The residue was extracted into hexanes (3 mL) and filtered. The filtrate was concentrated to \sim 1 mL and allowed to stand at $-35\text{ }^{\circ}\text{C}$ for 12 h to yield X-ray-quality crystals (27.0 mg, 0.036 mmol, 64.9%). Mp: 168–196 $^{\circ}\text{C}$ (decomp). ^1H NMR (25 $^{\circ}\text{C}$, 300.1 MHz, C_6D_6): δ 7.29–7.11 (m, 4H, $\text{NC}_5\text{H}_3/\text{C}_6\text{H}_3$), 6.98–6.82 (m, 5H, C_6H_3), 6.77 (t, $^3J_{\text{H-H}} = 7.5$ Hz, 1H, C_6H_3), 6.49 (d, $^3J_{\text{H-H}} = 8.1$ Hz, 1H, NC_5H_3), 6.30 (s, 1H, NH), 5.87 (d, $^3J_{\text{H-H}} = 7.0$ Hz, 1H, NC_5H_3), 3.24 (br, 2H, $\text{CH}(\text{CH}_3)_2$), 2.66 (br, 2H, Sc– $\text{CH}_2\text{--NC}_5\text{H}_3$), 2.19 (s, 7H, $\text{C}_6\text{H}_3\text{--CH}_3/\text{PCH}(\text{CH}_3)_2$), 2.04–1.84 (m, 3H, $\text{PCH}(\text{CH}_3)_2$), 1.70 (s, 3H, $\text{NC}_5\text{H}_3\text{--CH}_3$), 1.44–0.64 (m, 36H, $\text{PCH}(\text{CH}_3)_2/\text{CH}(\text{CH}_3)_2$). $^{13}\text{C}\{^1\text{H}\}$ NMR (25 $^{\circ}\text{C}$, 75.5 MHz, C_6D_6): δ 169.4 (s, NC_5H_3), 160.4 (d, C_6H_3), 159.4 (d, C_6H_3), 157.9 (s, NC_5H_3), 151.1 (s, C_6H_3), 136.8 (s, NC_5H_3), 135.5 (br, C_6H_3), 132.8 (s, NC_5H_3), 132.7 (s, C_6H_3), 132.6 (s, C_6H_3), 126.8 (d, C_6H_3), 123.2 (s,

C₆H₃), 120.8 (d, C₆H₃), 120.0 (d, C₆H₃), 119.2 (d, C₆H₃), 119.0 (d, C₆H₃), 117.2 (s, C₆H₃), 117.0 (s, C₆H₃), 110.9 (s, NC₅H₃), 57.4 (br, Sc-CH₂-NC₅H₃), 32.1 (s, CH₃-NC₅H₃), 28.0 (br, anilide CH-(CH₃)₂), 26.2 (d, CH(CH₃)₂), 25.7 (s, CH(CH₃)₂), 25.1 (s, CH(CH₃)₂), 23.1 (d, CH(CH₃)₂), 12.3–19.9 (m, CH(CH₃)₂/CH(CH₃)₂/Ar-CH₃), 19.5 (s, CH(CH₃)₂), 19.1 (s, CH(CH₃)₂), 18.6 (d, CH(CH₃)₂), 16.9 (d, CH(CH₃)₂). One PNP resonance and one pyridyl resonance were obscured by residual solvent. ³¹P{¹H} NMR (25 °C, 162.0 MHz, C₆D₆): δ 5.6 (Δν_{1/2} = 96.7 Hz), 3.6 (Δν_{1/2} = 102.0 Hz). IR (KBr): ν_{NH} 3315 cm⁻¹.

Kinetic Studies. The reaction of **1** to give **2** was monitored by ¹H NMR spectroscopy. The rate constant (*k*_{obs}) for the decay of **1** was measured by the integration of two separate resonances over time, the N–H resonance of the anilide group (s, 6.01 ppm) and the Sc–CH₃ resonance (t, 0.29 ppm), using as an external reference a capillary containing 1,4-dioxane in C₆D₆. The rate constant was measured every 5 °C over the range 35–75 °C, with triplicate runs at each temperature. This yielded six separate measurements for each temperature (triplicate runs for both N–H and Sc–CH₃), and their average is shown in Table 1. To obtain *k*_{obs} at each temperature, a

Table 1. Rate Constants for the Reaction 1 → 2 over the Temperature Range 35–75 °C

<i>T</i> (°C)	actual <i>T</i> (°C)	<i>T</i> (K)	average <i>k</i> _{obs} (s ⁻¹)
75	76.91	350.06	6.29 × 10 ⁻³
70	72.19	345.34	3.75 × 10 ⁻³
65	67.07	340.22	2.25 × 10 ⁻³
60	61.96	335.11	1.34 × 10 ⁻³
55	56.64	329.79	9.88 × 10 ⁻⁴
50	51.72	324.87	5.17 × 10 ⁻⁴
45	46.61	319.76	3.64 × 10 ⁻⁴
40	41.99	315.14	3.26 × 10 ⁻⁴
35	36.77	309.92	1.83 × 10 ⁻⁴

second-order analysis was used. The decay of pyridine was followed by integrating the pyridine 2,6-protons (d, 8.56 ppm) over time. The concentration of **1** in these measurements was 0.15 M. At each temperature, the actual temperature of the probe was recorded using an ethylene glycol standard [*T* = (4.637 – Δ)/0.009967, where Δ = δ_{OH} – δ_{CH₂} for 100% ethylene glycol].

Single-Crystal X-ray Diffraction. The data collection was carried out using Mo Kα radiation (graphite monochromator) with a frame time of 5 s and a detector distance of 5.0 cm. A collection strategy was calculated and complete data to a resolution of 0.73 Å with a redundancy of 4 were collected using APEX2 software. Six sections of frames were collected with 0.50° φ and ω scans.²⁴ Data to a resolution of 0.77 Å were considered in the reduction. Final cell constants were calculated from the xyz centroids of 1859 strong reflections from the actual data collection after integration. The intensity data were corrected for absorption using SADABS.²⁵ Additional crystallographic details are available in the SI in the form of CIF files and a description of the data collection, solution, and refinement procedures for each structure.²²

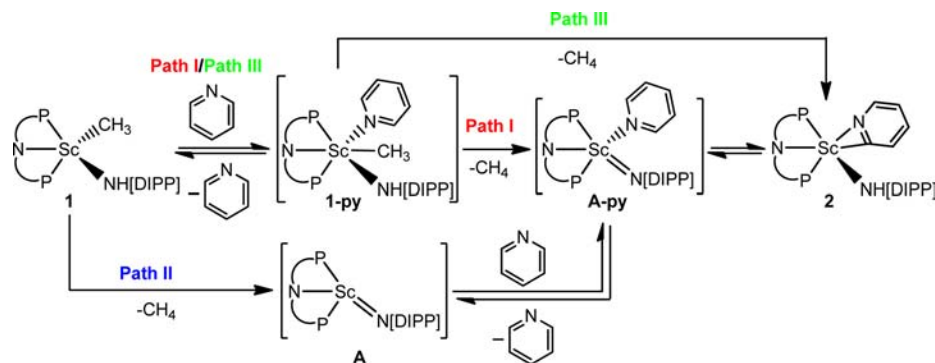
3. RESULTS AND DISCUSSION

Synthesis of Precursors to Scandium Imidos. Unlike early transition metals belonging to groups 4–6, the electro-positive nature coupled with the large ionic radius of the Sc³⁺ ion has made finding (or generating) terminal scandium imidos a challenging task.^{7–9,16} In most cases, oligomerization of the highly nucleophilic imide results in the formation of kinetically stable complexes.⁹ Teuben and Hessen's proposed transient monomeric scandium complex suggested that it was only a matter of ligand choice before a terminal imido of a rare-earth ion could be generated and investigated in detail.^{9a} In 2008, we

reported the first study to provide evidence for the existence of such species¹¹ via a series of trapping and deuteration studies using the robust and sterically encumbering pincer scaffold bis(2-diisopropylphosphino-4-tolyl)amide (PNP[−]), which was developed by Ozerov.²⁶ Soon after, Piers proposed a transient monomeric scandium imide intermediate formed via degradation of the imine residue of the β-diketiminato ligand.^{9b} Concurrent with our study, a terminal scandium imido formed using a cyclometalated species and a Lewis base was reported by Piers and co-workers.^{9c}

As reported in an earlier communication, the starting material (PNP)ScCl₂ can be readily prepared in 95% yield from Li(PNP) and ScCl₃(THF)₃ in toluene.^{13b} A close analogue of (PNP)ScCl₂ was previously described by Fryzuk using a more flexible and sterically encumbering PNP variant, [tBu₂PCH₂Si(Me)₂]₂N[−].²⁷ (PNP)ScCl₂ can be converted to (PNP)Sc(NH[DIPP])(CH₃) (**1**) via a series of transmetalation steps with LiNH[DIPP] and then LiMe.¹¹ Compound **1** is remarkably stable up to 50 °C over 24 h without significant evidence of decomposition. However, upon thermolysis of **1** at 70 °C in C₆(H/D)₆, **1** is completely consumed within 12 h, and multiple products are formed, one of which we identified as (PNP)Sc(NH[DIPP])(C₆H₅) on the basis of ³¹P and ¹H NMR spectroscopy via comparison to a sample independently prepared from (PNP)Sc(NH[DIPP])(Cl) and LiC₆H₅.^{11,22} Since α-hydrogen abstraction is likely the rate-determining step on the basis of kinetic studies performed for the neighboring complex (PNP)Ti=CH^tBu(R),¹⁹ we anticipated a much quicker reaction with more steric crowding in the departing alkyl group. Lowering the barrier to α-hydrogen abstraction could also disfavor other deleterious pathways. Accordingly, the metastable complex (PNP)Sc(NH[DIPP])(CH₂^tBu) and the stable complex (PNP)Sc(NH[DIPP])(CH₂SiMe₃) activate the C–H bond of benzene relatively cleanly under similar conditions (~70 °C). Using C₆D₆, we clearly showed that the NH[DIPP] ligand in (PNP)Sc(NH[DIPP])(CH₂^tBu) is converted to its isotopologue ND[DIPP], affording (PNP)Sc(ND[DIPP])(C₆D₅) with concurrent H₃C^tBu formation (Scheme 2).¹¹ Likewise, reactions to trap the elusive imido could be accomplished via the Tebbe and Schrock route: using AlMe₃ with **1** cleanly formed the imido zwitterion (PNP)Sc(μ₂-N[DIPP])(μ₂-CH₃)[Al(CH₃)₂] and CH₄ (Scheme 2).¹¹ This zwitterionic complex resembles the alkylidyne zwitterion (PNP)Ti(μ₂-C^tBu)(μ₂-CH₃)[Al(CH₃)₂] prepared analogously via treatment of (PNP)Ti=CH^tBu(CH₂^tBu) or (PNP)Ti=CH^tBu(C₆H₅) with AlMe₃.²⁸ To our surprise, however, we found that the AlMe₃ moiety of (PNP)Sc(μ₂-N[DIPP])(μ₂-CH₃)[Al(CH₃)₂] can be readily removed with excess pyridine to form the pyridyl–anilide complex (PNP)Sc(NH[DIPP])(η²-NC₅H₄) (**2**), which itself is a synthon of a terminal scandium imido complex, as shown via deuteration studies with pyridine-*d*₅ to form (PNP)Sc(ND[DIPP])(η²-NC₅D₄) (**2-d**₅) (Scheme 2). Likewise, complex **1** can also react rapidly with pyridine-*d*₅ to produce **2-d**₅.¹¹ In both cases, deuteration at the α-N of the anilide suggested that α-hydrogen abstraction precedes the C–H activation step, therefore discarding the more common σ-bond metathesis pathway generally associated with rare-earth metal or lanthanide C–H bond activation.^{29,30} This combination of results implied that a transient scandium imido likely was generated in all of these reactions [except for the reaction of **1** with Al(CH₃)₃]¹¹ and that the roles of the Lewis base and Lewis acid are critical in the α-hydrogen abstraction pathway.

Scheme 4. Proposed Paths for the Transformation of 1 into 2

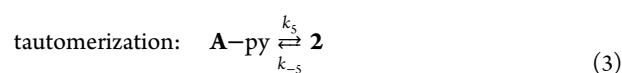
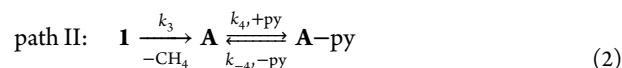
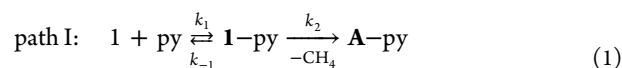


C–H Activation of Pyridine by a Transient Scandium Imido and Kinetic Isotope Effects. Previously, our group had established by isotope labeling studies that C–H activation of pyridine involves a transient scandium imido,^{3f,11} presumably via 1,2-C–H bond addition analogous to that in other reported imido systems.¹⁰ Since the ligands, PNP, and the peripherals of the anilide group are not deuterated, our isotopic labeling studies suggest that formation of the imido likely proceeds by one or a combination of the three paths shown in Scheme 4. Path I is analogous to that proposed for Chen and Cui's imidos^{2a,15d} in that the σ donor must first bind to Sc before the α -hydrogen abstraction proceeds. Path II is not Lewis base-induced but instead involves direct α -hydrogen abstraction, akin to the results of mechanistic studies provided by Bergman and Wolczanski on transient group 4 imides.^{10a,b,e–h} Path III involves a concerted step wherein C–H abstraction and C–H bond activation of pyridine occur in an asynchronous fashion without the need to form a Sc–N multiple bond. This last path is not to be confused with σ -bond metathesis involving only the methyl and *o*-pyridine protons, which is clearly not operative on the basis of isotopic labeling studies. Nevertheless, path III should still depend on a pre-equilibrium step involving pyridine binding. Distinguishing path III from path I or II might not be trivial because the role of pyridine and α -hydrogen abstraction may not be decoupled (interchange mechanism). However, paths I and II can be discriminated since the main difference is the role of pyridine in the reaction: binding occurs before or after methane release and imido formation, respectively.

Our group has also shown that pyridine-*d*₅ exchanges with 2 over 8 h at 90 °C to yield the isotopologue 2-*d*₅, hinting that the formation of the imide (PNP)Sc=N[DIPP](NC₅H₅) (A-py) is reversible, therefore discrediting path III (Scheme 4).¹¹ When 1 was treated with pyridine-*d*₅ at 35 °C and the rate compared with that for pyridine, a KIE of 1.1(2) was observed,²² indicating that C–H activation of pyridine is not rate-determining in the formation of the pyridyl. To establish whether α -hydrogen abstraction is the slow step, the isotopologue (PNP)Sc(ND[DIPP])(CH₃) (1-*d*₁) was prepared. At 35 °C, a KIE of 5.37(6) was observed for three independent runs ($k_{\text{avg}} = 3.41 \times 10^{-5} \text{ M}^{-1} \text{ s}^{-1}$). When the latter complex was heated to 50 °C, a KIE (or temperature-dependent or equilibrium KIE) of 4.9(14) compared with the rate for 1 → 2 was observed.²² The conversion of 1 to 2 (with concomitant release of CDH₃) without any deuterium incorporation into the anilide nitrogen also suggests α -hydrogen abstraction to be virtually irreversible under these conditions and argues against hypothetical σ -complex intermediates such as (PNP)Sc(N[DIPP])(σ -CDH₃) or (PNP)Sc-

(N[DIPP])(σ -CDH₃)(NC₅H₅) being stable or even present in significant quantities along the reaction coordinate to allow for exchange with the imide.^{19a,10m} This was verified by the fact that no isotope scrambling was observed when 1-*d*₁ was thermolyzed in deuterobenzene (3 days at 50 °C).²² The isotopologue (PNP)Sc(NH[DIPP])(CD₃) (1-*d*₃), which was synthesized from salt metathesis with LiNH[DIPP] and (PNP)Sc(CD₃)(I), also showed no evidence of isotopic scrambling upon thermolysis (3 days at 50 °C).²² In summary, our primary KIE data at 35 and 50 °C are consistent with α -hydrogen abstraction being overall-rate-determining and in accord with the formation of a scandium imido moiety. The data collected at 35 °C argue that equilibrium isotope effects do not make a major contribution to our values (see below). Our reported KIE is also consistent with those for other α -H-abstraction-based mechanisms reported with the pincer ligand PNP.¹⁹

Dependence on Pyridine. The role of pyridine in the formation of the scandium imide A-py is critical, since we,¹¹ Chen,^{2a,15a–c} Cui,^{15d} and recently Piers^{9c} have relied on a Lewis base of this type presumably to promote α -hydrogen abstraction. For this reason, we explored the role of pyridine in the conversion of 1 to 2. From our proposed set of paths described in Scheme 4, we can differentiate I from II via kinetic analysis of the reaction. For instance, path I invokes a pre-equilibrium between 1 and pyridine ($K_{\text{eq}1} = k_1/k_{-1}$) to generate the intermediate (PNP)Sc(NH[DIPP])(CH₃)(py) (1-py), which then decomposes with rate constant k_2 to generate A-py and methane (eq 1). Path II relies on the loss of methane from 1 with rate constant k_3 to generate unsaturated imido intermediate A, which should bind pyridine reversibly to form A-py ($K_{\text{eq}4} = k_4/k_{-4}$; eq 2). On the basis of our KIE for pyridine/pyridine-*d*₅ (see above), A-py should be in equilibrium with 2 in the post-rate-determining step ($K_{\text{eq}5} = k_5/k_{-5}$; eq 3). However, at room temperature, this equilibrium should heavily favor 2, as it is the only species observed spectroscopically. As a result, eq 3 should not be part of our rate expressions derived using eqs 1 and 2.



By applying the pre-equilibrium approximation to path I, we obtained the rate expression $d[2]/dt = k_{\text{obs}}[1][\text{py}]$, with $k_{\text{obs}} = K_{\text{eq}}k_2$.²² According to this analysis, if C–H activation of pyridine occurs via path I, we should observe a first-order dependence on pyridine and a first-order dependence on I. Likewise, for path I, as the concentration of pyridine approaches infinity, the rate equation should then simplify to $d[2]/dt = k'_2[1]$, where $k'_2 = k_2[\text{py}]_0$ (i.e., pseudo-first-order kinetics). Since path II does not involve a pre-equilibrium step, we had to invoke the steady-state approximation, from which the rate equation $d[2]/dt = k_3[1]$ was obtained.²² For this path, the rate of the reaction should be independent of the pyridine concentration. However, this analysis holds true only if there are no other intermediates in solution. In addition to the absence of side products, our plot in Figure 1 shows that the decay of 1 and the formation of 2 were clean, without any side reactions or detectable intermediates, as judged by ¹H or ³¹P NMR spectroscopy.

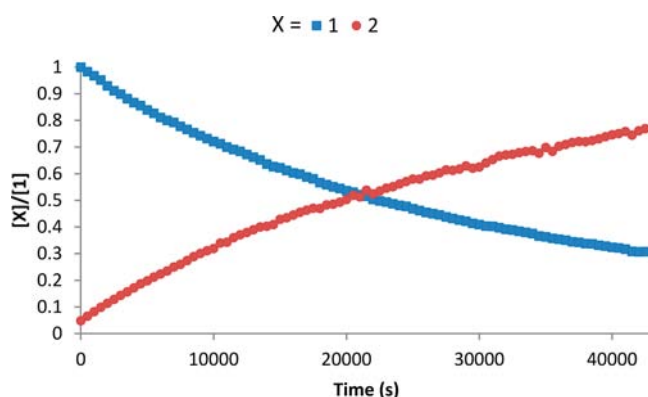


Figure 1. Plot showing the decay of 1 and formation of 2 at 40 °C (obtained by monitoring the N–H resonances of 1 and 2). Kinetic data for only ~ 2 half-lives ($t_{1/2} = 5.8$ h) are shown. The reaction was complete after ~ 36 h.

If the reaction is zeroth order in substrate [as in the proposed path II or our (PNP)Ti(IV) alkyidyne system, (PNP)Ti \equiv C^tBu],¹⁹ then a plot of $[\text{py}]$ versus time would exhibit a linear dependence. Alternatively, if the reaction is first order in substrate, a plot of $\ln[\text{py}]$ versus time would be linear. When we plotted both $[\text{py}]$ versus time and $\ln[\text{py}]$ versus time, we observed nonlinear fits (Figures 2 and 3). However, when a second-order plot $[\ln([\text{py}]/[1])]$ vs time was used, a linear relationship ($R^2 = 0.998$) was observed (Figure 4); to ensure consistency in our measurements, both the N–H and Sc–CH₃ protons were monitored to determine the concentration of 1. Thus, our data are more in accord with the reaction being first order in pyridine and first order in 1 (i.e., path I).

The strongest evidence that path I is the most likely route was observed when we examined the effect of the pyridine concentration on the rate of the reaction. To determine more precisely the role of pyridine in the reaction, we conducted concentration-dependent studies of the overall rate of the 1 \rightarrow 2 conversion with $[\text{py}]$ ranging from 0.07 to 1.0 M using C₆D₆ and NC₅D₅.²² As shown in Figure 5 and Table 2, the rate of the reaction decayed as the concentration of pyridine was decreased. No saturation effect was observed, which is inconsistent with path II.

Finally, to lend further support to the mechanism proposed in path I, we examined evidence for the existence of the

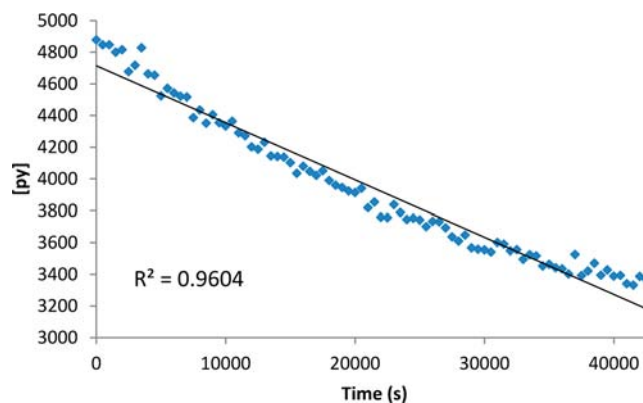


Figure 2. Zeroth-order plot with respect to pyridine for the 1 \rightarrow 2 transformation. The pyridine concentration was determined by monitoring the integral of the NMR peak for the pyridine 2,6-protons. The reaction was conducted at 40 °C.

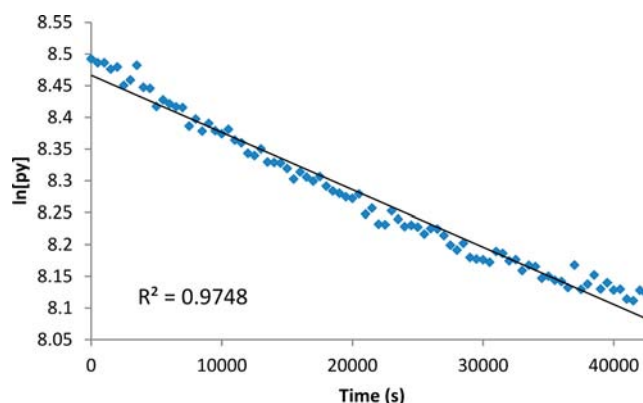


Figure 3. First-order plot with respect to pyridine for the 1 \rightarrow 2 transformation. The pyridine concentration was determined by monitoring the integral of the NMR peak for the pyridine 2,6-protons. The reaction was conducted at 40 °C.

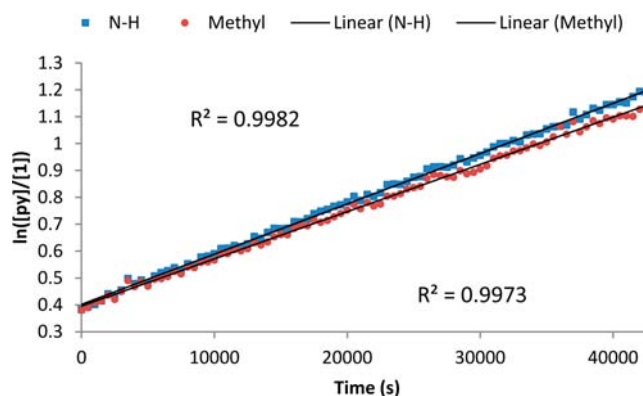


Figure 4. Second-order plot with respect to pyridine for the 1 \rightarrow 2 transformation. The pyridine concentration was determined by monitoring the integral of the NMR peak for the pyridine 2,6-protons, and the concentration of 1 was determined by monitoring the integrals of both the Sc–NH and Sc–CH₃ resonances. The reaction was conducted at 40 °C.

intermediates I-py, A-py, and A. To that end, a solution of 1 and pyridine in toluene-*d*₈ was cooled to -60 °C in order to decrease the rate of binding of pyridine, which would allow us to observe the adduct I-py or the product arising from α -hydrogen abstraction. Unfortunately, no evidence for I-py was

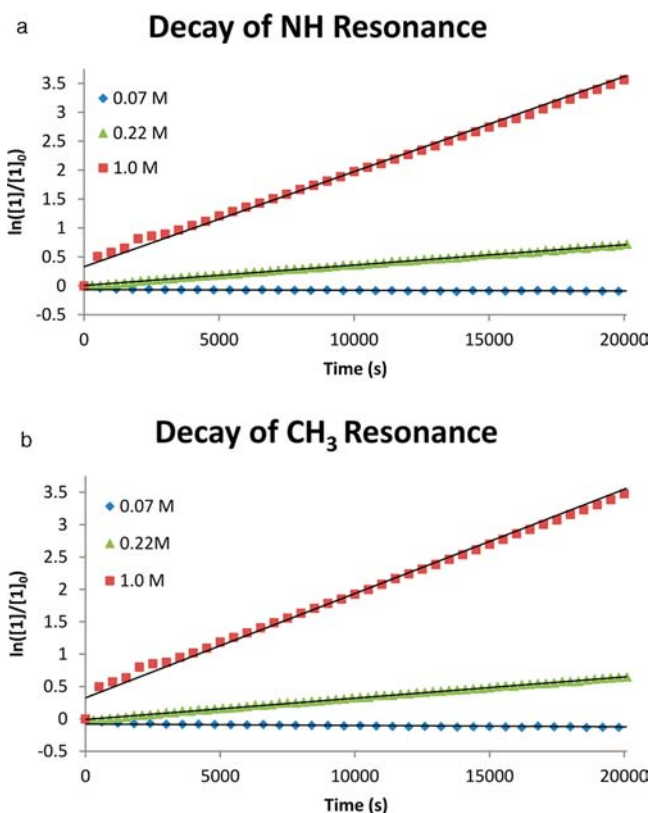


Figure 5. Plots showing the pyridine concentration dependence of the rate of the **1** → **2** conversion. The top plot was obtained by monitoring the decay of the anilide N–H ¹H NMR resonance of **1**, and the bottom plot was obtained by monitoring the decay of the Sc–CH₃ ¹H NMR resonance of **1**. [**1**]₀ = 0.15 M in both plots.

Table 2. Values of *k*_{obs} Showing the Pyridine Concentration Dependence of the Rate of the **1** → **2** Conversion at 35 °C

[py] (M)	<i>k</i> _{obs} (s ^{−1})
0.07	1.42 × 10 ^{−6}
0.22	3.74 × 10 ^{−5}
1.0	1.62 × 10 ^{−4}
5.0	8.63 × 10 ^{−4}
10.0	2.66 × 10 ^{−3}

detected by either ¹H or ³¹P NMR spectroscopy, and the direct observation of A-py or A was futile, as both intermediates occur after the α-hydrogen abstraction step, which is overall-rate-determining. Spectroscopic observation of such an intermediate might be compromised by the fact that such species would have spectroscopic signatures very similar to that of **1**. However, indirect evidence for formation of A-py was observed by the thermolysis of (PNP)Sc(ND[DIPP])(η²-NC₅H₄) (**2-d**₁), the isotopologue of complex **2** containing ~75% deuterium incorporation at the anilide position (Scheme 5). Complex **2-d**₁ was prepared from (PNP)Sc(ND[DIPP])(Cl) and Li-(NC₅H₄) at −100 °C.³¹ The amount of proton/deuterium incorporation in **2-d**₁ was determined by monitoring the integrals of the N–H resonance and the proton resonances of the pyridyl moiety. After 2 days at room temperature in C₆D₆, there was no change in the integrals of the anilide resonance (6.18 ppm, ~0.36H) and the resonances of the 3- and 6-protons on the pyridyl ring (7.77 and 8.33 ppm, respectively, each resonance being a doublet integrating to 1.0H; Scheme 5),

but after the complex was heated at 60 °C for 9 days, the integrals of the anilide resonance and the pyridyl proton resonance at 8.33 ppm had equilibrated to 0.75H and 0.67H, respectively, with the integral of the pyridyl resonance at 7.77 ppm remaining at 1.0H. This exchange provides hard evidence that A-py is accessible but formed *slowly* at higher temperatures and that the imido is not accessible at room temperature, consistent with the observed reactivity of complex **1**.

To probe the possibility of the formation of A from **1**, complex **1** was thermolyzed at 70 °C in C₆D₆ in the absence of other substrates such as pyridine. After 12 h, **1** was completely consumed, and the reaction afforded several products, including (PNP)Sc(NH[DIPP])(C₆H₅) [or, when C₆D₆ was used, (PNP)Sc(ND[DIPP])(C₆D₅)] as the major product.¹¹ As a result, we cannot completely refute path **II** as a competing reaction coordinate taking place at higher temperatures. However, in the presence of pyridine, complex **2** is formed quantitatively (as determined by ¹H and ³¹P NMR spectroscopy) with a *t*_{1/2} of 17.8 min at 70 °C, suggesting that path **II** is unfeasible at room temperature or in the time frame for completion of the reaction at higher temperatures. Although path **II** has analogous precedent in our group when the alkylidyne precursor (PNP)Ti≡CH^tBu(R) (R[−] = CH₃, CH₂^tBu, CH₂SiMe₃, C₆H₅) was used,¹⁹ path **I** is more likely for a reaction involving a donor substrate because of the vacant coordination site available in **1** coupled with the much larger ionic radius of Sc³⁺ (74.5 pm) compared with Ti⁴⁺ (60.5 pm).^{17a} This path would also be more in accord with the necessity of a Lewis base in the formation of Chen and Cui's scandium imides.^{2a,15}

Activation Parameters for the Formation of a Transient Scandium Imide. Since our system follows a second-order rate expression, we can monitor the decays of both **1** and pyridine over time. The integrated rate law expressed in a linear form is shown in eq 4.

$$\ln\left(\frac{[\mathbf{1}]_0[\text{py}]}{[\text{py}]_0[\mathbf{1}]}\right) = \frac{k_{\text{obs}}}{[\text{py}]_0 - [\mathbf{1}]_0}t \quad (4)$$

By monitoring the decays of both **1** and pyridine, we determined the rate constant of the reaction at different temperatures, thereby allowing us to obtain values of the activation parameters. Accordingly, from the Eyring plot in Figure 6 we were able to extract a Δ*H*[‡] value of 17.9(9) kcal/mol, which is lower than those for Wolczanski's imido system, (tBu₃SiNH)₂Zr=NSi^tBu₃ [25.9(4) kcal/mol],^{10h} and our group's alkylidyne system, (PNP)Ti≡C^tBu [24(7) kcal/mol].^{19d,f} This lower enthalpy of activation could translate into the transition state of **1**-py (**1**-py-TS) being relatively early, with both the N–H and Sc–CH₃ bonds being essentially preserved. The same type of transition state was observed in the calculated pathway for the **2** → A-py tautomerization (see below). In the case of Δ*G*[‡], however, the **1** → **2** conversion yielded an estimated value of 23.5 kcal/mol at 308.15 K, which is comparable to those for (tBu₃SiNH)₃Zr(CH₃) → (tBu₃SiND)₃Zr(C₆D₅) (~28.5 kcal/mol at 308.15 K)^{10h} and (PNP)Ti≡CH^tBu(CH₂^tBu) → (PNP)Ti≡CD^tBu(C₆D₅) (~24.6 kcal/mol at 308.15 K).^{19d,f} The reason why the Gibbs free energy of our (PNP)Sc=N[DIPP] system is comparable to those of Wolczanski's zirconium imido and our titanium alkylidyne, despite its much lower enthalpy of activation, is that the scandium system has a negative *entropy* of activation [Δ*S*[‡] = −18(3) cal/(mol K)]. In fact, the entropic component accounts

Scheme 5. Isotopic Labeling Studies Showing the Formation of the Imide Adduct A-py upon Heating at 60 °C for 9 days (Red Spectrum, $t = 0$; Blue Spectrum, $t = 9$ days at 60 °C)

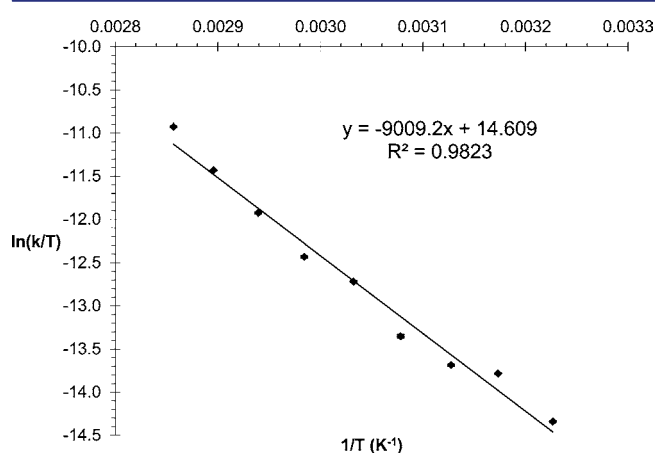
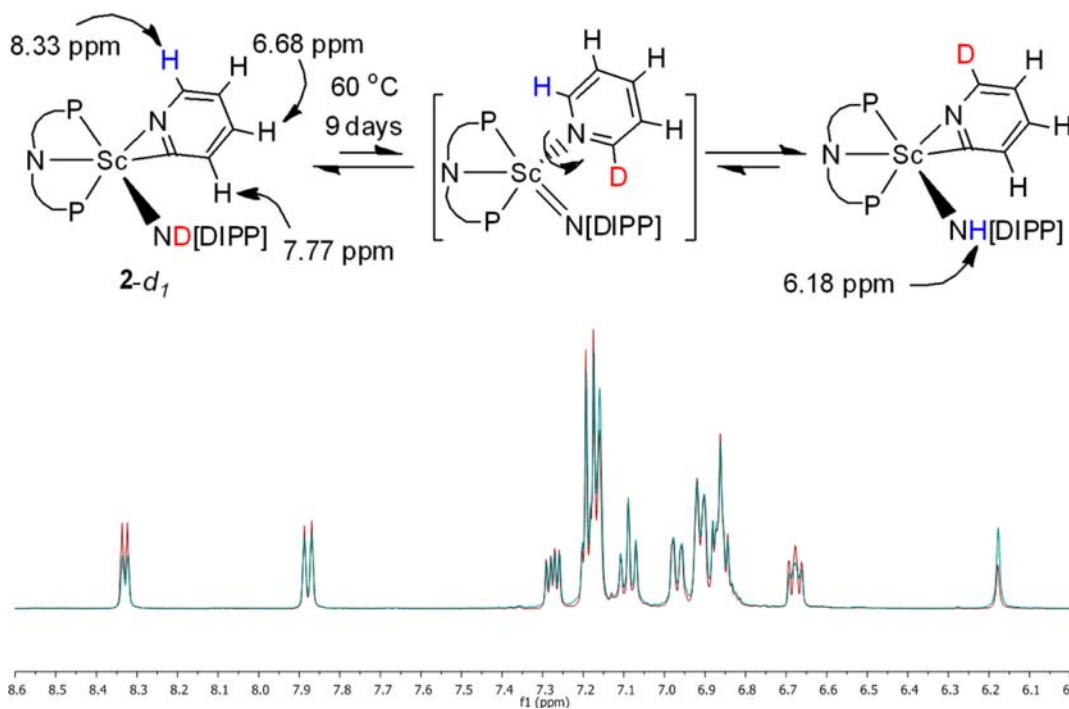
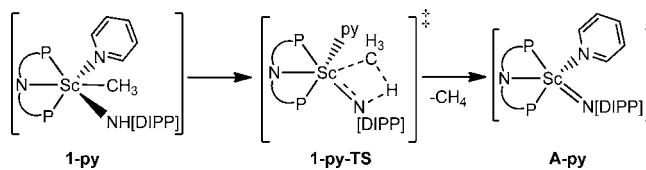


Figure 6. Eyring plot for the $1 \rightarrow 2$ transformation in C_6D_6 over the temperature range 35–74 °C.

for almost 24% of the total Gibbs free energy, which is consistent with a highly ordered transition state along the reaction coordinate. Both the zirconium and titanium systems mentioned are zeroth order in substrate, so their major entropic penalty is likely due to alignment in the molecule to allow for α -proton abstraction [$-7(1)$ cal/(mol K) for Zr;^{10h} $-2(3)$ cal/(mol K) for Ti^{19d,f}].

Our highly negative ΔS^\ddagger is consistent with an associative process involving the binding of pyridine to **1** to promote the release of methane concomitant with formation of the imido, which most likely is A-py. The highly negative ΔS^\ddagger also suggests a highly constrained geometry preceding methane elimination, which likely involves the four-centered transition state 1-py-TS shown in Scheme 6. We assume that the role of pyridine is to coordinate to the scandium metal center in order to induce more steric crowding, which would place the methyl moiety closer to the departing H^+ of the anilide, but pyridine

Scheme 6. Proposed Transition State Involved in the Formation of the Imido A-py from 1-py



might play a dual role, as it could also behave as a Brønsted base that promotes H^+ transfer to the methyl. This mechanism, though, is disfavored because the rate of activation of 2-substituted pyridines is lower than that of unsubstituted pyridine (DMAP > 4-picoline > pyridine > 2-picoline > 2-iminopyridine or 2,6-lutidine; see below).

To understand further the steps involving pyridine binding, α -hydrogen abstraction, and pyridine C–H bond activation, we can break the pathway into two distinct stages. The first stage involves the conversion of **1** to the imido A-py via pyridine binding and subsequent α -hydrogen abstraction, while the second is the tautomerization of A-py to give **2**. This second step is what can allow for the formation of **2-d₅** from **2**, and it also permits the study of the C–H bond activation event without too much entropic dominance. Consequently, the profile of the tautomerization step was calculated using density functional theory. Calculations at the B3LYP/LACVP** level were performed to elucidate the reaction profile but also to discard other plausible mechanistic scenarios not involving the formation of a scandium imido (A-py or A).²²

Figure 7 depicts the most likely reaction profile for the formation of the imide A-py via a tautomerization step involving the pyridyl complex **2**. As anticipated, the resting state in complex **2** has the hydrogen atom of the anilide nitrogen pointed away from the Sc–C bond of the pyridyl ligand (**2-anti**). This orientation is consistent with the X-ray

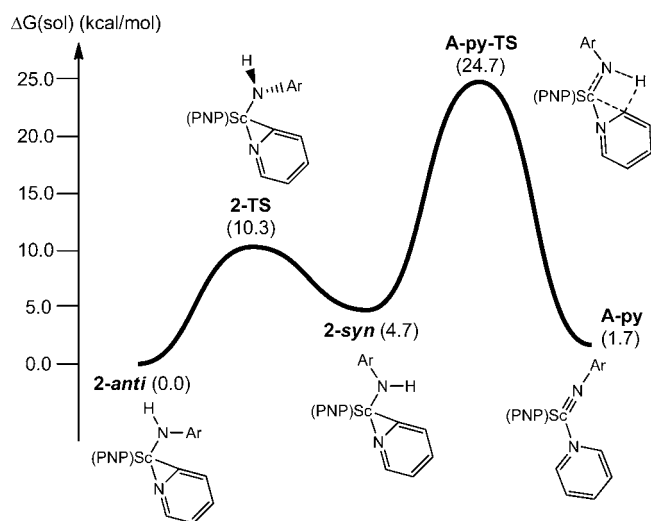


Figure 7. Computed reaction coordinate for the $2 \rightarrow \text{A-py}$ tautomerization. The rest of the reaction coordinate is not shown since it represents the microscopic reverse, $\text{A-py} \rightarrow 2$.

structure of **2** previously reported by our group as well as the X-ray structure of **1**.¹¹ Prior to tautomerization, rotation of the Sc–N bond occurs (with a small penalty of 10.3 kcal/mol) in order to align the N–H bond with the basic pyridyl carbon (**2-syn**). The barrier for this step mainly arises from the large steric repulsion between the DIPP ring and the isopropyl groups of the PNP ligand in the transition state **2-TS**, wherein the anilide hydrogen is rotated to give a H–N–Sc–C torsion angle of 105.6° instead of the more planar values of 173.0° for **2-anti** and 4.1° for **2-syn**. The computed Sc–N_{anilide} bond distances in **2-anti** (2.066 Å) and **2-syn** (2.057 Å) are similar to those found in other Sc–N_{anilide} complexes (~2.07 Å). In the computed structure of **2-TS**, the Sc–P distances of 2.751 and 2.779 Å are slightly longer than those in complex **2** [2.7251(10) and 2.7397(10) Å], which supports our assertion that steric clashing among these groups likely disfavors one isomer relative to the other.

In addition to a small barrier for isomerization, the rotamer **2-syn** is slightly endergonic by 4.7 kcal/mol, which implies that fast interconversion of these species takes place at room temperature. However, the slow step in our reaction coordinate is the tautomerization involving **2-syn** and **A-py**. Intramolecular α -hydrogen migration costs an additional 20.0 kcal/mol (24.7 kcal/mol overall from **2-anti**). As a result, the latter step is rate-determining, akin to the formation of **2** from **1-py**. The computed transition state involved in the tautomerization step, **A-py-TS**, involves a four-centered species in which the migrating hydrogen is locked between the imide nitrogen and the pyridyl carbon. The computed bond distances are consistent with an early transition state. The Sc–N_{imide} bond distance for **A-py-TS** is computed to be 1.907 Å, which is close to the Sc–N_{anilide} distance reported for the AlMe₃-trapped imido complex (PNP)Sc(μ_2 -N[DIPP])(μ_2 -CH₃)[Al(CH₃)₂] [1.9366(14) Å] and the Sc–N_{anilide} bond distances of anilide complexes (~2.07 Å). However, this distance is slightly longer than the Sc=NAr distances observed in the structurally characterized imidos reported by Chen [1.881(5) and 1.8591(18) Å].^{2a,15b} The Sc–C bond distance in **A-py-TS** (2.520 Å) is rather long compared with both the average Sc–C_{pyridyl} bond distance (~2.22 Å)^{3f,11,14,31,32} and the Sc–CH₃ bond length in (PNP)Sc(μ_2 -N[DIPP])(μ_2 -CH₃)[Al(CH₃)₂]

[2.385(2) Å].¹¹ The transferred proton in **A-py-TS** is about halfway between the pyridyl carbon and the imido nitrogen (H–N_{imide}, 1.342 Å; H–C_{pyridyl}, 1.454 Å), indicating the TS to be at the midway point between **A-py** and **2-syn**.

A-py has a similar energy to **2**, being only 1.7 kcal/mol higher in energy than **2-anti**, which implies that this species is relatively stable. Figure 7 does not depict the entire energy diagram involving equilibration of **A-py** back to **2**, since this involves the microscopic reverse (and hence, **A-py** is not isolable). Although **A-py** is expected to be thermodynamically stable relative to **2-syn**, the energy required to form this species results in the overall re-formation of **2-syn** and ultimately **2-anti** by virtue of microscopic reversibility. This type of tautomerization (at temperatures high enough to overcome the thermodynamic barrier) has been exploited by our group to generate iminopyridine ligands, in some cases catalytically.^{3f} The most notable feature of the reaction profile shown in Figure 7 is the optimized computed structure of the imido **A-py**. This putative intermediate has a seemingly short Sc=N bond length of 1.84 Å, and the Sc–N–C_{ipso} angle is 169.7°. The short bond length and large bond angle imply that the Sc=N[DIPP] bond should actually be considered as a Sc≡N[DIPP] bond (Figure 7), in agreement with the bond distance of 1.90 Å computed for a Sc–N triple bond using the method put forth by Pauling (eq 5),^{17b}

$$D_{\text{Sc-N}} = r_{\text{Sc}} + r_{\text{N}} - c|\chi_{\text{Sc}} - \chi_{\text{N}}| \quad (5)$$

where $D_{\text{Sc-N}}$ is the bond distance, c is the Schomaker–Stevenson coefficient, and r_i and χ_i are the covalent radius and electronegativity, respectively, of atom i . Using eq 5, we obtained a bond distance of 1.98 Å for a Sc–N double bond (slightly longer than the Sc=N[DIPP] bond distance of 1.94 Å in (PNP)Sc(μ_2 -N[DIPP])(μ_2 -CH₃)[Al(CH₃)₂]) and a bond distance of 2.06 Å for a Sc–N single bond (similar to the observed average bond distance of 2.06 Å for our Sc–N_{anilide} bonds). Additionally, these computed metrical parameters are comparable to those for Chen's structurally characterized scandium imide [Sc–N = 1.881(5) and 1.8591(18) Å and Sc–N–C_{ipso} = 169.6(5)° and 167.90(17)°, respectively].^{2a,15b} The evidence that Sc–N multiple bonding in **A-py** takes place is further augmented by the two orthogonal Sc–N π molecular orbitals HOMO and HOMO–2 shown in Figure 8. These orbitals suggest the imido ligand in complex **A-py** to be the most basic site. The calculated Mayer bond order (MBO) of the imido intermediate (1.56) is consistent with a Sc–N interaction between those of a double bond and a triple bond²¹ and is similar to the MBO of 1.41 for the related phosphinidene complex (PNP)Sc(μ_2 -P[DMP])(μ_2 -Br)[Li(THF)₂] (DMP =

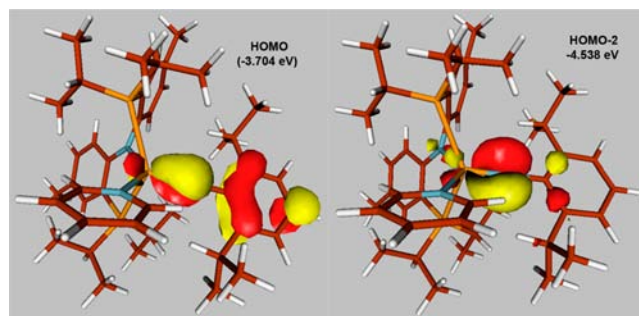


Figure 8. Most important frontier orbitals for the computed structure of **A-py**. Isodensity is shown at 0.05 au.

2,6-dimesitylphenyl), which also exhibits a pseudo-triple-bond interaction.^{13e}

Complexes bearing a scandium–ligand multiple bond have been reported for ligands containing phosphorus, the heavier congener of nitrogen.^{13e} Our phosphinidene-ate complex (PNP)Sc(μ_2 -P[DMP])(μ_2 -Br)[Li(THF)₂], which contains the same (PNP)Sc(III) framework, also shows pseudo-triple-bond character between scandium and phosphorus, albeit more polarized toward the phosphorus.^{13e} In the present case, however, the imido moiety in A-py undergoes 1,2-C–H bond addition across the scandium–nitrogen multiple bond, and this is presumably due to the better overlap of the smaller, harder nitrogen atom with the rare-earth ion's less diffuse 3d orbitals. In contrast, (PNP)Sc(μ_2 -P[DMP])(μ_2 -Br)[Li(THF)₂] engages in group transfer reactions, although the reaction of the phosphinidene complex with pyridine leads to decomposition, resulting the formation of several products that we have been unable to characterize.^{13e} Such a contrast might be due to the fact that the phosphinidene complex has an inert bromide ion coordinating where the pyridine would have to bind to allow for a 1,2-addition reaction. Additionally, the HOMO of (PNP)Sc(μ_2 -P[DMP])(μ_2 -Br)[Li(THF)₂] is orthogonal to the plane of the substrate (enforced by the bulky DMP group) (Figure 9), whereas the HOMO of A-py is directed toward the C–H bond of pyridine, which facilitates the bond activation step (Figure 8).

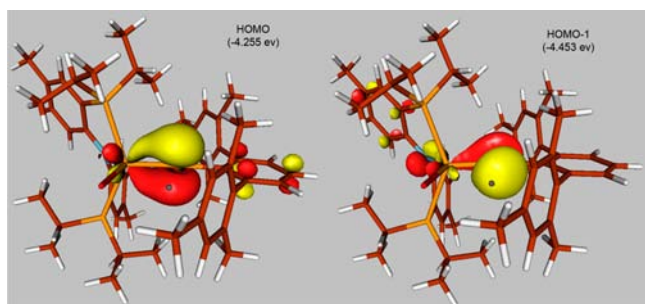
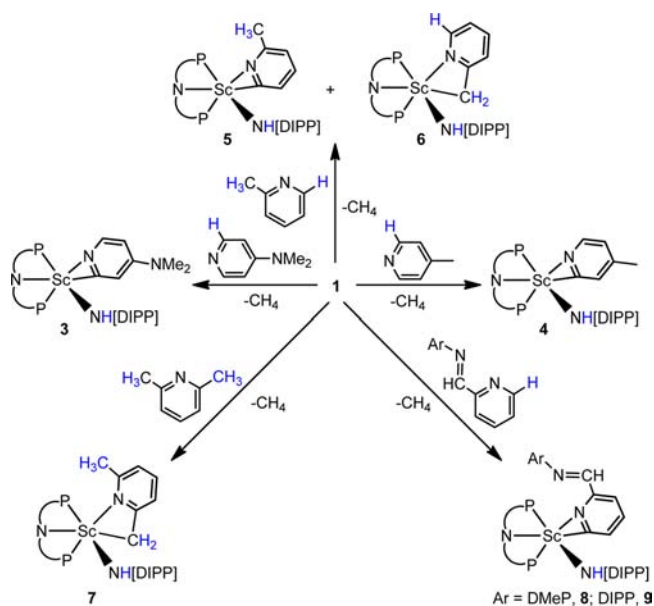


Figure 9. Most important frontier orbitals for the computed structure of (PNP)Sc(μ_2 -P[DMP])(μ_2 -Br)[Li(THF)₂].^{13e} The Li ion and THF ligands have been omitted for clarity. Isodensity is shown at 0.05 au.

Effect of Other Pyridine Substrates on the Overall Rate of the Reaction. We examined the effect of substituted pyridine rings in the C–H bond activation step. According to our proposed path I, the binding of pyridine to **1** promotes the loss of methane to form A-py, which then promotes C–H activation at the 2-position of pyridine to generate **2**. Since pyridine does have an effect on the C–H abstraction step and is clearly involved in the TS leading to **2**, we thermolyzed **1** with various substituted pyridines to observe their effect on the rate.

Accordingly, when DMAP was added to **1** in C₆D₆ and the mixture was monitored over time, the reaction was complete within 30 min ($k = 1.25 \times 10^{-2} \text{ M}^{-1} \text{ s}^{-1}$ at 50 °C) and yielded the 4-*N,N*-dimethylaminopyridyl complex (PNP)Sc(NH[DIPP])(η^2 -NC₅H₃-4-NMe₂) (**3**) quantitatively (Scheme 7). The connectivity in complex **3** was established on the basis of a combination of ¹H, ¹³C, and ³¹P NMR spectral data. For example, the ¹H NMR spectrum revealed the anilide N–H resonance at 6.01 ppm, while the dimethylamino group showed one singlet at 2.31 ppm consistent with a fluxional –NMe₂ group. The [DIPP] aryl group exhibited slow rotation relative to the NMR time scale due to the sterically hindered

Scheme 7. Reactions of **1** with Substituted Pyridines To Form Complexes **3–9**



environment around the metal. This was indicated by a broad methyne proton (3.43 ppm) and two isopropyl methyl doublets (1.36 and 1.33 ppm, ²J_{HH} = 6.8 Hz) in the ¹H NMR spectrum. The ¹³C NMR spectrum was consistent with a pyridyl carbon at 213.8 ppm (broad), and the ³¹P NMR spectrum exhibited two resonances at 3.8 and 4.4 ppm, analogous to those of other scandium complexes having a pyridyl moiety. The salient NMR resonances of **3** and other complexes are summarized in Table 3.

Table 3. Salient NMR Spectroscopic Signatures (in ppm) of ¹H, ³¹P, and ¹³C Nuclei for Complexes **1–9**

complex	N–H	PNP	α -C
1 ^a	6.01	4.2; 2.5	30.4 (CH ₃)
2 ^a	6.18	4.5; 5.1	217.2 (pyridyl)
3	6.01	3.8; 4.4	213.8 (pyridyl)
4	6.16	3.9; 4.7	216.0 (pyridyl)
5	6.08	4.8; 5.6	216.9 (pyridyl)
6	6.17	4.8; 5.6	53.3 (CH ₂)
7	6.30	3.6; 5.6	57.4 (CH ₂)
8 ^b	6.34	4.8; 6.1	216.0 (pyridyl)
9 ^b	6.28	4.0; 5.9	215.4 (pyridyl)

^aData from ref 11. ^bData from ref 3f.

The reaction of 4-methylpyridine with **1** to generate (PNP)Sc(NH[DIPP])(η^2 -NC₅H₃-4-Me) (**4**) (Scheme 7; $k = 1.05 \times 10^{-3} \text{ M}^{-1} \text{ s}^{-1}$ at 50 °C) was an order of magnitude slower than the DMAP reaction but faster than C–H bond activation by pyridine to yield **2** ($k = 5.13 \times 10^{-4} \text{ M}^{-1} \text{ s}^{-1}$ at 50 °C). The ¹H NMR spectrum of **4** had features similar to those of other C–H-activated pyridine products including the anilide proton (6.16 ppm), the [DIPP] group exhibiting hindered rotation (ⁱPr-methine: 3.40 ppm, broad; ⁱPr-methyl: 1.36 ppm, virtual triplet from two overlapping doublets, ³J_{H–H} = 6.4 Hz), and asymmetric PNP tolyl groups (2.18 and 2.23 ppm). The ³¹P NMR spectrum of complex **4** was also consistent with this assignment, having two resonances at 3.9 and 4.7 ppm. Lastly,

the pyridyl carbon appeared in the ^{13}C NMR spectrum at 216.0 ppm. Akin to complex 2, single-crystal X-ray diffraction analysis of complex 4 revealed a pseudo-octahedral Sc(III) ion having an η^2 -bound pyridyl ligand [Sc1–N2, 2.192(2) Å; Sc1–C27, 2.216(2) Å] and an anilide ligand [Sc1–N3, 2.0497(18) Å]. No α -H agostic interaction of the isotropically refined anilide hydrogen (Sc1...H4, 2.363 Å) was observed, and the anilide hydrogen points away from the pyridyl carbon (Figure 10).

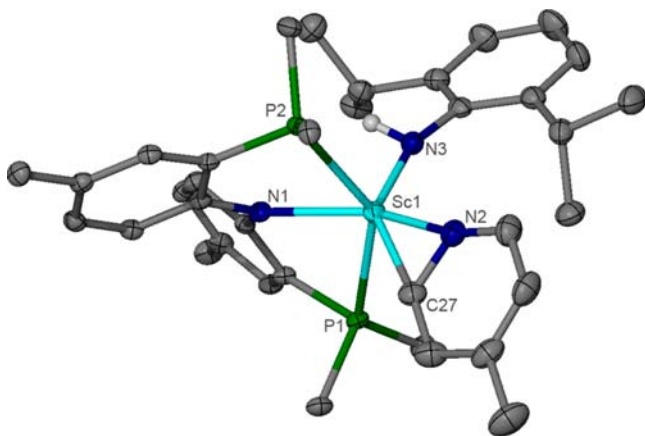


Figure 10. Molecular structure of 4 with thermal ellipsoids at the 50% probability level. ^iPr methyl groups on the PNP ligand, solvent molecules, and H atoms (except for the α -hydrogen on N3) have been omitted for clarity. Selected distances (Å) and angles (deg): Sc1–N1, 2.338(7); Sc1–C43, 2.720(5); Sc1–C44, 2.391(4); N3–C39, 1.355(10); N3–C43, 1.377(8); C43–C44, 1.408(7); Sc1–N2–C27, 73.14(14); N2–C27–Sc1, 71.21(13); Sc1–N3–C_{ipso}, 160.64(17); P1–Sc1–P2, 142.40(3).

When pyridine was substituted at the 4-position, the C–H activation occurred at the 2-position, analogous to the case for pyridine, albeit more rapidly for better σ donors. However, when the pyridine was substituted at the 2-position, divergent reactivity was observed. As anticipated for a more hindered Lewis base, the reaction of 1 with 2-picoline ($k = 5.7 \times 10^{-5} \text{ M}^{-1} \text{ s}^{-1}$ at 50 °C) was much slower than that of unsubstituted pyridine even though the $\text{p}K_{\text{a}}$ is higher than that of pyridine. Only minimal reactivity was observed after 4 h at 50 °C. This lack of reactivity is presumably due to the more sterically crowded Lewis base. Regardless, when the mixture was heated at 70 °C for 36 h, complex 1 was fully consumed as assayed by ^{31}P NMR spectroscopy. To our surprise, however, there were two separate anilide N–H resonances (6.08 and 6.17 ppm), indicating that two products were formed. On the basis of the integration of these resonances, the ratio of products was 46:54. Further heating of the mixture did not alter the ratio of the two products, suggesting that they were not equilibrating. Although two products were observed in the ^1H NMR spectrum, there was no evidence of multiple products in the ^{31}P NMR spectrum. The ^{31}P NMR spectra of the two compounds were close to coincidental, showing two broad resonances at 4.8 ppm ($\nu_{1/2} = 118 \text{ Hz}$) and 5.6 ppm ($\nu_{1/2} = 132 \text{ Hz}$) similar to those of 1 (4.5 and 5.1 ppm). The peak width at half height ($\Delta\nu_{1/2}$) for these resonances was broader than normal (80–90 Hz), which is the only indication in the ^{31}P NMR spectrum that there were two overlapping resonances. A Sc–C_{py} ^{13}C resonance was observed at 216.9 ppm, indicating that one of the complexes was the expected C–H-activated product. Interestingly, when a 135° distortionless enhancement by

polarization transfer (DEPT-135) NMR experiment was run on the mixture, an oppositely phased signal was observed at 53.3 ppm,²² indicating the presence of a CH_2 moiety. This would be possible only if the methyl group of 2-picoline had been activated. This feature, along with the presence of the o -H resonance observed as a doublet at 7.75 ppm ($^3J_{\text{HH}} = 7.1 \text{ Hz}$), led us to conclude that one of the products was derived from C–H bond activation at the 2-methyl carbon while the other product was a pyridyl product analogous to 2 (Scheme 7). On the basis of a combination of multinuclear NMR spectroscopic data, we determined that the two products produced from C–H bond activation were the complexes (PNP)Sc(NH[DIPP])-(η^2 -NC₅H₃-2-CH₃) (5) and (PNP)Sc(NH[DIPP])(κ^2 -C,N-NC₅H₄-2-CH₂) (6) (Scheme 7).²² Although the mixture of complexes was inseparable because of their similar solubilities, we resorted to single-crystal X-ray diffraction studies to establish conclusively the site of C–H bond activation and the binding mode of the pyridine motif in compound 6. To our surprise, complex 5 cocrystallized with 6 in a $\sim 30:70$ ratio in the solid state (Figure 11).

The PNP and anilide ligands in 6 and 5 are virtually crystallographically equivalent. The only disorder occurs in the picoline ligand, and it is due to the two binding modes (η^2 and η^3) shown in Figure 11, which are averaged over the entire lattice.²² This allows for the direct measurement of both the sp^2 and sp^3 C–H activated products of the reaction of 2-picoline. Since complexes 5 and 6 cocrystallized, their metrical parameters correspond to the average values for the two complexes [Sc1–N1, 2.190(2) Å; Sc1–N2, 2.059(2) Å; Sc1–P1, 2.7337(7) Å; Sc1–P2, 2.7086(11) Å; P1–Sc1–P2, 144.60(3)°; Sc1–N2–C_{ipso}, 158.22(19)°]. Given that the disorder is centered around the activated 2-picoline, the products corresponding to the different activation sites are labeled separately in each structural diagram. The major component, 6, has the picoline atoms labeled with just a number, while those in the minor component, 5, are designated with a D after the atom number (i.e., N3 for the picoline nitrogen in 6 and N3D for the same nitrogen in 5). Even though the solid-state X-ray structure of 5 resembles the geometrical features observed in 2 and 4 [Sc1–N3D, 2.186(14) Å; Sc1–C39D, 2.176(10) Å],¹¹ the structure of complex 6 differs significantly. First, the coordinated pyridine group [Sc1–N3, 2.338(7) Å] is intact, with activation of the C–H bond in this case occurring at the 2-CH₃ position. The binding mode of the picolyl ligand in 6 appears to be η^3 (Figure 11 right), although the Sc1–C43 bond distance of 2.720(5) Å is longer than those of other crystallographically characterized allyl species (avg Sc–C_{AC} distance = 2.44 Å, where C_{AC} denotes the central allylic carbon).^{33,34} This bond distance, however is within the range observed for scandium–arene interactions (2.50–2.84 Å).³⁵ Presumably, the steric clash between the picoline ring and the isopropyl groups of the PNP ligand prevents the full allyl-type interaction. The dual reactivity of 2-picoline is unique, because in general, C–H bond activation of pyridine occurs in the sp^2 -CH and not the sp^3 -CH position in picolines.^{33,36} Only in rare cases has activation of only the methyl C–H bonds been observed.^{33,36b}

To probe further the impact of the sterics at the 2- and 6-positions on the rate of substrate activation, 1 was reacted with 2,6-lutidine, which was expected to interact with the metal center significantly less than the other substrates while maintaining a basicity similar to those of the other pyridine derivatives. Accordingly, when 1 was allowed to react with 2,6-

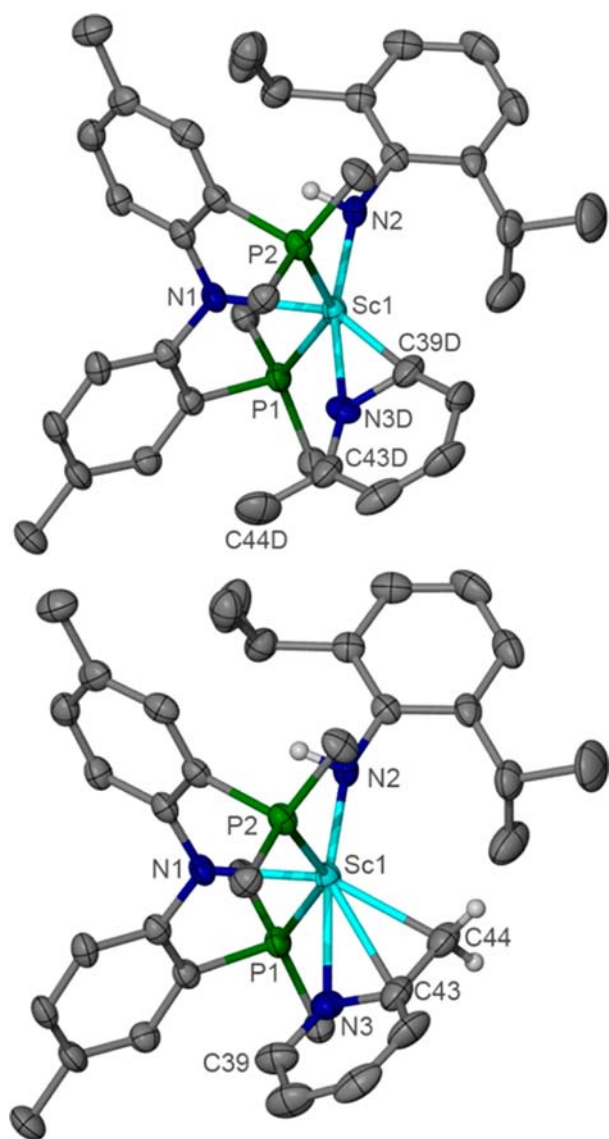
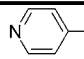
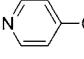
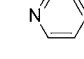
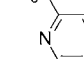
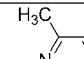
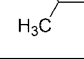
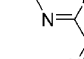


Figure 11. Molecular structures of (top) **5** and (bottom) **6** with thermal ellipsoids at the 50% probability level. ⁱPr methyl groups on the PNP ligand, solvent molecules, and H atoms (except for the α -hydrogen on N2) have been omitted for clarity. Selected distances (Å) and angles (deg) for **5**: Sc1–N3D, 2.186(14); Sc1–C39D, 2.176(10); N3D–C39D, 1.370(17); N3D–C43D, 1.369(15); C43D–C44D, 1.423(14); Sc1–N3D–C39D, 71.3(7); N3D–C39D–Sc1, 72.1(7). For **6**: Sc1–N3, 2.338(7); Sc1–C43, 2.720(5); Sc1–C44, 2.391(4); N3–C39, 1.355(10); N3–C43, 1.377(8); C43–C44, 1.408(7); N3–C43–C44–Sc1, 31.3.

lutidine at room temperature, the reaction was >40% complete after 10 days. Under thermolytic conditions (65 °C), the reaction reached completion, generating the complex (PNP)-Sc(NH[DIPP])(κ^2 -C,N-NC₅H₃-2-CH₂-6-CH₃) (**7**), which shares some similar NMR spectral features with complex **6** (Scheme 7).²² The ³¹P NMR spectrum showed two resonances at 3.6 and 5.6 ppm similar to the ones observed for the **5/6** mixture (4.8 and 5.6 ppm). Also, the DEPT-135 NMR spectrum exhibited a resonance at 57.4 ppm,²² consistent with activation of one of the lutidine methyl groups.^{30,33,36} This α -carbon resonance corresponded by heteronuclear multiple-bond coherence (HMQC) to the broad proton resonance at 3.24 ppm.²² The unactivated methyl resonance of lutidine was

also observed in the ¹H NMR spectrum (singlet at 1.70 ppm), albeit significantly downfield-shifted from that of free lutidine (2.35 ppm), and the anilide proton was observed as well (6.30 ppm). The fact that this reaction was so slow ($t_{1/2}$ >10 days) supports our assertion that the pyridine binds the metal center before methane loss and imido formation. This also disfavors a proton shuttling mechanism, as the steric bulk of the lutidine would have a much less pronounced effect on its ability to deprotonate. This reactivity is consistent with our proposal that the pyridine substrate must bind to the metal center before the complex releases methane and forms the imido, since among the substituted pyridines presented here, DMAP is the most basic [pK_a values: pyridine, 5.23; 4-picoline, 5.99; 2-picoline, 6.00; 2,6-lutidine, 6.65; 4-aminopyridine (instead of DMAP), 9.11] and therefore the most nucleophilic.³⁷ Notably, the stronger the Lewis base, the swifter the α -hydrogen abstraction, unless the base is too sterically hindered. This was also observed with our previously reported activation of iminopyridines.^{36,7b} At room temperature, less than 5% of **1** was converted to the iminopyridine adduct. However, at 70 °C, the reaction was complete in 14 h. Table 4 summarizes the rates

Table 4. Rates Measured at 50 °C for the Conversion of **1** to Its Respective C–H-Activated Products Using Various Substituted Pyridines

Substrate	Complex Formed from 1	k (M ⁻¹ s ⁻¹) at 50 °C
	3	1.25×10^{-2}
	4	1.05×10^{-3}
	2	5.13×10^{-4}
	5 and 6	5.7×10^{-5}
	7	$< 10^{-5}$, $t_{1/2}$ >10 days
	8	$< 10^{-5}$, $t_{1/2}$ >10 days
	9	$< 10^{-5}$, $t_{1/2}$ >10 days

measured for the conversion of **1** to the respective C–H activation products obtained using various substituted pyridines. It is quite possible that the formation of complexes **5–7** proceeds via an unsaturated imide **A** (or a mixture of **A** and **A**-substrate, where the substrate is 2-picoline or 2,6-lutidine), given the higher temperatures needed. This might help explain why two C–H bond activation products were observed in the case of 2-picoline.

The reaction of **1** with 2-fluoropyridine was unfortunately very slow and yielded several products that were detected by ^1H and ^{31}P NMR spectroscopy.²² We found that complex **1** also reacts with other σ donors, such as triethylamine (TEA), trimethylphosphine, quinuclidine, and 2,2'-bipyridine, but lamentably, these reactions yielded multiple (PNP)Sc(III) products that precluded definitive characterization. Resonances in the anilide N–H region of the ^1H NMR spectrum that could not be attributed to the starting material **1** were observed for these reactions, indicating that C–H activation likely occurred in parallel with other competing reactions.

4. CONCLUSIONS

In this work, we have shown that the Sc(III) scaffold (PNP)Sc can support a terminal imido group. However, the reactive nature of the imide results in C–H bond activation of a substrate such as pyridine. In the absence of a Lewis base, activation of the solvent (C_6H_6) occurs, albeit sluggishly and not cleanly. We have also demonstrated that a Lewis base such as pyridine (or a close derivative thereof) promotes α -hydrogen abstraction in complex **1**. The Lewis base with the lowest $\text{p}K_{\text{a}}$ results in the fastest α -hydrogen abstraction. We propose the role of the pyridine to be twofold: (i) binding of the Lewis base forces the methyl and primary anilide to be closer in space, therefore lowering the barrier for proton transfer, and (ii) the pyridine ligand allows for convenient trapping of the polarized basic imide group, resulting in the formation of a pyridyl ligand by 1,2-C–H bond addition. Evidence for direct participation of pyridine (as a Brønsted base) in the proton transfer was disproved by the fact that bulkier substrates such as 2-picoline and 2,6-lutidine retarded the α -hydrogen abstraction. As a result, our proposed pathway proceeds via an associative-type mechanism in which scandium imide formation most likely involves a pre-equilibrium step between **1** and the pyridine adduct **1-py**, followed by the α -hydrogen abstraction step, which is overall-rate-determining. Although the imido moiety can be accessed at higher temperatures without the aid of a donor such as pyridine, this leads to multiple products and occurs over a longer time frame than the C–H activation of pyridine at the same temperature.

Via a deuteration study, we have shown indirectly that the microscopic reverse reaction, the formation of **A-py** from **2**, occurs slowly at higher temperatures. As shown previously with Sc(III), the phosphine arms of the PNP ligand can be hemilabile,¹⁴ which could allow for binding of more sterically encumbered pyridine derivatives such as 2,6-lutidine and 2-iminopyridines. At present, we cannot discard the possibility that at least one phosphine pendant group dissociates during the binding of the Lewis base or that it even promotes H^+ transfer. Kinetic isotope effects strongly imply imido formation and loss of methane to be the slow step, as opposed to C–H bond activation of pyridine. The present work has also provided the first evidence of aliphatic C–H activation by a scandium imido, since complex **1** can indiscriminately activate the methyl group of 2-picoline versus the ortho position. Likewise, the methyl group of 2,6-lutidine can be activated, albeit sluggishly. Although complex **2** can tautomerize to **A-py**, attempts to observe chemistry reminiscent of an imido (metathesis or imide group transfer) were compromised by the reactive nature of the pyridyl Sc–C bond.

■ ASSOCIATED CONTENT

Supporting Information

X-ray crystallographic information (CIF), isotopic and kinetic studies, kinetic analysis, and spectral data. This material is available free of charge via the Internet at <http://pubs.acs.org>.

■ AUTHOR INFORMATION

Corresponding Author

mindiola@indiana.edu

Present Addresses

[†]Dalian Institute of Chemical Physics, Chinese Academy of Sciences, Dalian 116023, China.

[‡]Department of Chemistry and Chemical Engineering, Royal Military College of Canada, Kingston, Ontario, Canada K7K 7B4.

Notes

The authors declare no competing financial interest.

■ ACKNOWLEDGMENTS

Financial support of this research was provided by the National Science Foundation (CHE-0848248 and CHE-1152123). J.S. acknowledges postdoctoral financial support from NSERC, and M.G.C. acknowledges CONACYT for a postdoctoral fellowship.

■ REFERENCES

- (1) For reviews, see: (a) Wigley, D. E. *Prog. Inorg. Chem.* **1994**, *42*, 239. (b) Nugent, W. A.; Haymore, B. L. *Coord. Chem. Rev.* **1980**, *31*, 123. (c) Cummins, C. C. *Prog. Inorg. Chem.* **1998**, *47*, 685. (d) Hazari, N.; Mountford, P. *Acc. Chem. Res.* **2005**, *38*, 839. (e) Berry, J. F. *Comments Inorg. Chem.* **2009**, *30*, 28. (f) Mehn, M. P.; Peters, J. C. *J. Inorg. Biochem.* **2006**, *100*, 634. (g) Sharp, P. R. *Comments Inorg. Chem.* **1999**, *21*, 85. (h) Smith, J. M. *Comments Inorg. Chem.* **2008**, *29*, 189. (i) Abu-Omar, M. M. *Dalton Trans.* **2011**, *40*, 3435. (j) Fout, A. R.; Kilgore, U. J.; Mindiola, D. J. *Chem.—Eur. J.* **2007**, *13*, 9428. (k) Cundari, T. R. *J. Am. Chem. Soc.* **1992**, *114*, 7879. (l) Eikey, R. A.; Abu-Omar, M. M. *Coord. Chem. Rev.* **2003**, *243*, 83. (m) Mindiola, D. J. *Acc. Chem. Res.* **2006**, *39*, 813. (n) Mindiola, D. J.; Bailey, B. C.; Basuli, F. *Eur. J. Inorg. Chem.* **2006**, 3135. (o) Che, C. M. *Pure Appl. Chem.* **1995**, *67*, 225. (p) Zarubin, D. N.; Ustynyuk, N. A. *Russ. Chem. Rev. (Engl. Transl.)* **2006**, *75*, 671. (q) Nugent, W. A.; Mayer, J. M. In *Metal–Ligand Multiple Bonds*; Wiley-Interscience: New York, 1988. (r) Holland, P. L. *Acc. Chem. Res.* **2008**, *41*, 905.
- (2) Examples of terminal imidos at the extreme ends of the transition metal series (group 3 and groups 8 and 9) have been reported. See: (a) Lu, E.; Li, Y.; Chen, Y. *Chem. Commun.* **2010**, *46*, 4469. (b) Efremenko, I.; Poverenov, E.; Martin, J.; Milstein, D. *J. Am. Chem. Soc.* **2010**, *132*, 14886. (c) Poverenov, E.; Efremenko, I.; Frenkel, A.; Ben-David, Y.; Shimon, L. J. W.; Leitun, G.; Konstantinovski, L.; Martin, J.; Milstein, D. *Nature* **2008**, *455*, 1093. (d) Mindiola, D. J.; Hillhouse, G. L. *J. Am. Chem. Soc.* **2001**, *123*, 4623. (e) Laskowski, C. A.; Miller, A. J. M.; Hillhouse, G. L.; Cundari, T. R. *J. Am. Chem. Soc.* **2011**, *133*, 771. (f) Waterman, R.; Hillhouse, G. L. *J. Am. Chem. Soc.* **2008**, *130*, 12628. (g) Waterman, R.; Hillhouse, G. L. *J. Am. Chem. Soc.* **2003**, *125*, 13350. (h) Laskowski, C. A.; Hillhouse, G. L. *Organometallics* **2009**, *28*, 6114. (i) Harrold, N. D.; Waterman, R.; Hillhouse, G. L.; Cundari, T. R. *J. Am. Chem. Soc.* **2009**, *131*, 12872. (j) Kogut, E.; Wiencko, H. L.; Zhang, L.; Cordeau, D. E.; Warren, T. H. *J. Am. Chem. Soc.* **2005**, *127*, 11248. (k) Wiese, S.; McAfee, J. L.; Pahls, D. R.; McMullin, C. L.; Cundari, T. R.; Warren, T. H. *J. Am. Chem. Soc.* **2012**, *134*, 10114. (l) Bai, G.; Stephan, D. W. *Angew. Chem., Int. Ed.* **2007**, *46*, 1856. (m) Ackermann, L. *Organometallics* **2003**, *22*, 4367. (n) Lorber, C.; Choukroun, R.; Vendier, L. *Organometallics* **2004**, *23*, 1845. A copper nitrene dimer and transient monomer have been

reported. See: (o) Badiei, Y. M.; Krishnaswamy, A.; Melzer, M. M.; Warren, T. H. *J. Am. Chem. Soc.* **2006**, *128*, 15056.

(3) (a) Duncan, A. P.; Bergman, R. G. *Chem. Rec.* **2002**, *2*, 431. (b) Odom, A. L. *Dalton Trans.* **2005**, 225. (c) Thomson, R. K.; Bexrud, J. A.; Schafer, L. L. *Organometallics* **2006**, *25*, 4069. (d) Eisenberger, P.; Schafer, L. L. *Pure Appl. Chem.* **2010**, *82*, 1503. (e) Mendiola, D. J. *Comments Inorg. Chem.* **2008**, *29*, 73. (f) Wicker, B. F.; Scott, J.; Fout, A. R.; Maren, P.; Mendiola, D. J. *Organometallics* **2011**, *30*, 2453. (g) Cantrell, G. K.; Meyer, T. Y. *J. Am. Chem. Soc.* **1998**, *120*, 8035. (h) Pohlki, F.; Doye, S. *Chem. Soc. Rev.* **2003**, *32*, 104. (i) Bytschkov, I.; Doye, S. *Eur. J. Org. Chem.* **2003**, 935. (j) Pohlki, F.; Doye, S. *Angew. Chem., Int. Ed.* **2001**, *40*, 2305. (k) Anderson, L. L.; Schmidt, J. A. R.; Arnold, J.; Bergman, R. G. *Organometallics* **2006**, *25*, 3394. (l) Hill, J. E.; Proffitt, R. D.; Fanwick, P. E.; Rothwell, I. P. *Angew. Chem., Int. Ed. Engl.* **1990**, *29*, 713.

(4) For other selected examples of imides used in catalysis, see: (a) Anderson, L. L.; Arnold, J.; Bergman, R. G. *Org. Lett.* **2004**, *6*, 2519. (b) Cao, C.; Shi, Y.; Odom, A. L. *J. Am. Chem. Soc.* **2003**, *125*, 2880. (c) Li, Y.; Shi, Y.; Odom, A. L. *J. Am. Chem. Soc.* **2004**, *126*, 1794. (d) Shi, Y.; Ciszewski, J. T.; Odom, A. L. *Organometallics* **2001**, *20*, 3967. (e) Vujkovic, N.; Ward, B. D.; Maisee-François, A.; Wadepohl, H.; Mountford, P.; Gade, L. H. *Organometallics* **2007**, *26*, 5522. (f) Bolton, P. D.; Mountford, P. *Adv. Synth. Catal.* **2005**, *347*, 355. (g) Ong, T.-G.; Yap, G. P. A.; Richeson, D. S. *Organometallics* **2002**, *21*, 2839. (h) Dubberly, S. R.; Friedrich, A.; Willman, D. A.; Mountford, P.; Radius, U. *Chem.—Eur. J.* **2003**, *9*, 3634. (i) Roizen, J. L.; Harvey, M. E.; Du Bois, J. *Acc. Chem. Res.* **2012**, *45*, 911. (j) Du Bois, J.; Tomooka, C. S.; Hong, J.; Carreira, E. M. *Acc. Chem. Res.* **1997**, *30*, 364. (k) Muñiz, K. *Chem. Soc. Rev.* **2004**, *33*, 166. (l) Romão, C. C.; Kühn, F. E.; Herrmann, W. A. *Chem. Rev.* **1997**, *97*, 3197. (m) Müller, T. E.; Hultsch, K. C.; Yus, M.; Foubelo, F.; Tada, M. *Chem. Rev.* **2008**, *108*, 3795. (n) Majumder, S.; Gipson, K. R.; Staples, R. J.; Odom, A. L. *Adv. Synth. Catal.* **2009**, *351*, 2013. (o) Vujkovic, N.; Fillol, J. L.; Ward, B. D.; Wadepohl, H.; Mountford, P.; Gade, L. H. *Organometallics* **2008**, *27*, 2518. (p) Leung, S. K.-Y.; Tsui, W.-M.; Huang, J.-S.; Che, C.-M.; Liang, J.-L.; Zhu, N. *J. Am. Chem. Soc.* **2005**, *127*, 16629. (q) Walsh, P. J.; Baranger, A. M.; Bergman, R. G. *J. Am. Chem. Soc.* **1992**, *114*, 1708. (r) McGrane, P. L.; Jensen, M.; Livinghouse, T. J. *J. Am. Chem. Soc.* **1992**, *114*, 5459. (s) Johnson, J. S.; Bergman, R. G. *J. Am. Chem. Soc.* **2001**, *123*, 2923. (t) Lian, B.; Spaniol, T. P.; Horrillo-Martínez, P.; Hultsch, K. C.; Okuda, J. *Eur. J. Inorg. Chem.* **2009**, 429. (u) Ruck, R. T.; Zuckerman, R. L.; Krska, S. W.; Bergman, R. G. *Angew. Chem., Int. Ed.* **2004**, *43*, 5372. (v) Aneetha, H.; Basuli, F.; Bollinger, J.; Huffman, J. C.; Mendiola, D. J. *Organometallics* **2006**, *25*, 2402. (w) King, E. R.; Hennessy, E. T.; Betley, T. A. *J. Am. Chem. Soc.* **2011**, *133*, 4917.

(5) (a) Schrock, R. R. *Chem. Rev.* **2009**, *109*, 3211. (b) Wright, W. R. H.; Batsanov, A. S.; Messinis, A. M.; Howard, J. A. K.; Tooze, R. P.; Hanton, M. J.; Dyer, P. W. *Dalton Trans.* **2012**, *41*, 5502. (c) La Pierre, H. S.; Arnold, J.; Toste, F. D. *Angew. Chem., Int. Ed.* **2011**, *50*, 3900. (d) Bolton, P. D.; Mountford, P. *Adv. Synth. Catal.* **2005**, *347*, 355. (e) Coles, M. P.; Dalby, C. I.; Gibson, V. C.; Clegg, W.; Elsegood, M. R. *J. Chem. Soc., Chem. Commun.* **1995**, 1709. (f) Coles, M. P.; Gibson, V. C. *Polym. Bull.* **1994**, *33*, 529. (g) Nomura, K. In *New Developments in Catalysis Research*; Bevy, L. P., Ed.; Nova Science Publishers: New York, 2005; p 199. (h) Nomura, K.; Zhang, W. *Chem. Sci.* **2010**, *1*, 161. (i) Nomura, K.; Sagara, A.; Imanishi, Y. *Macromolecules* **2002**, *35*, 1583. (j) Wang, W.; Nomura, K. *Macromolecules* **2005**, *38*, 5905. (k) Wang, W.; Nomura, K. *Adv. Synth. Catal.* **2006**, *348*, 743. (l) Onishi, Y.; Katao, S.; Fujiki, M.; Nomura, K. *Organometallics* **2008**, *27*, 2590. (m) Zhang, S.; Katao, S.; Sun, W.-H.; Nomura, K. *Organometallics* **2009**, *28*, 5925.

(6) Basuli, F.; Aneetha, H.; Huffman, J. C.; Mendiola, D. J. *J. Am. Chem. Soc.* **2005**, *127*, 17992.

(7) (a) Mendiola, D. J.; Scott, J. *Nat. Chem.* **2011**, *3*, 15. (b) Scott, J.; Mendiola, D. J. *Dalton Trans.* **2009**, 8463.

(8) Giesbrecht, G. R.; Gordon, J. C. *Dalton Trans.* **2004**, 2387.

(9) (a) Beetstra, D. J.; Meetsma, A.; Hessen, B.; Teuben, J. H. *Organometallics* **2003**, *22*, 4372. Another example of a bridging imido

was recently reported. See: (b) Conroy, K. D.; Piers, W. E.; Parvez, M. *Organometallics* **2009**, *28*, 6228. (c) Chu, T.; Piers, W. E.; Dutton, J. L.; Parvez, M. *Organometallics* **2012**, DOI: 10.1021/om300913d.

(10) (a) Walsh, P. J.; Hollander, F. J.; Bergman, R. G. *J. Am. Chem. Soc.* **1988**, *110*, 8729. (b) Cummins, C. C.; Baxter, S. M.; Wolczanski, P. T. *J. Am. Chem. Soc.* **1988**, *110*, 8731. (c) Royo, P.; Sánchez-Nieves, J. J. *Organomet. Chem.* **2000**, *597*, 61. (d) De With, J.; Horton, A. D. *Angew. Chem., Int. Ed. Engl.* **1993**, *32*, 903. (e) Hoyt, H. M.; Bergman, R. G. *Angew. Chem., Int. Ed.* **2007**, *46*, 5580. (f) Cundari, T. R.; Klinckman, T. R.; Wolczanski, P. T. *J. Am. Chem. Soc.* **2002**, *124*, 1481. (g) Schaller, C. P.; Bonanno, J. B.; Wolczanski, P. T. *J. Am. Chem. Soc.* **1994**, *116*, 4133. (h) Schaller, C. P.; Cummins, C. C.; Wolczanski, P. T. *J. Am. Chem. Soc.* **1996**, *118*, 591. (i) Hanna, T. E.; Keresztes, I.; Lobkovsky, E.; Bernskoetter, W. H.; Chirik, P. J. *Organometallics* **2004**, *23*, 3448. (j) Walsh, P. J.; Hollander, F. J.; Bergman, R. G. *Organometallics* **1993**, *12*, 3705. (k) De With, J.; Horton, A. D.; Orpen, A. G. *Organometallics* **1993**, *12*, 1493. (l) De With, J.; Horton, A. D.; Orpen, A. G. *Organometallics* **1990**, *9*, 2207. (m) Schafer, D. F.; Wolczanski, P. T. *J. Am. Chem. Soc.* **1998**, *120*, 4881.

(11) Scott, J.; Basuli, F.; Fout, A. R.; Huffman, J. C.; Mendiola, D. J. *Angew. Chem., Int. Ed.* **2008**, *47*, 8502.

(12) Labinger, J. A.; Bercaw, J. E. *Nature* **2002**, *417*, 507.

(13) (a) Masuda, J. D.; Jantunen, K. C.; Ozerov, O. V.; Noonan, K. J. T.; Gates, D. P.; Scott, B. L.; Kiplinger, J. L. *J. Am. Chem. Soc.* **2008**, *130*, 2408. (b) Scott, J.; Fan, H.; Wicker, B. F.; Fout, A. R.; Baik, M.-H.; Mendiola, D. J. *J. Am. Chem. Soc.* **2008**, *130*, 14438. (c) Cui, P.; Chen, Y.; Xu, X.; Sun, J. *Chem. Commun.* **2008**, 5547. (d) Zimmermann, M.; Takats, J.; Kiel, G.; Törnroos, K. W.; Anwander, R. *Chem. Commun.* **2008**, 612. (e) Wicker, B. F.; Scott, J.; Andino, J. G.; Gao, X.; Park, H.; Pink, M.; Mendiola, D. J. *J. Am. Chem. Soc.* **2010**, *132*, 3691. (f) Mills, D. P.; Soutar, L.; Lewis, W.; Blake, A. J.; Liddle, S. T. *J. Am. Chem. Soc.* **2010**, *132*, 14379. (g) Fustier, M.; Le Goff, X. F.; Le Floch, P.; Mezailles, N. *J. Am. Chem. Soc.* **2010**, *132*, 13108. (h) Zimmermann, M.; Rauschmaier, D.; Eichele, K.; Törnroos, K. W.; Anwander, R. *Chem. Commun.* **2010**, *46*, 5346. (i) Cui, P.; Chen, Y.; Borzov, M. V. *Dalton Trans.* **2010**, *39*, 6886. (j) Korobkov, I.; Gambarotta, S. *Organometallics* **2009**, *28*, 5560. (k) Zhang, W.-X.; Wang, Z. T.; Nishiura, M.; Xi, Z. F.; Hou, Z. M. *J. Am. Chem. Soc.* **2011**, *133*, 5712. (l) Liddle, S. T.; Mills, D. P.; Wooley, A. J. *Chem. Soc. Rev.* **2011**, *40*, 2164. In the gas phase, lanthanide compounds having metal–ligand multiple bonds have been detected. See: (m) Gong, Y.; Wang, X.; Andrews, L.; Chen, M.; Dixon, D. A. *Organometallics* **2011**, *30*, 4443.

(14) Wicker, B. F.; Pink, M.; Mendiola, D. J. *Dalton Trans.* **2011**, *40*, 9020.

(15) (a) Lu, E.; Zhou, Q.; Li, Y.; Chu, J.; Chen, Y.; Leng, X.; Sun, J. *Chem. Commun.* **2012**, *48*, 3403. (b) Lu, E.; Chu, J.; Chen, Y.; Borzov, M. V.; Li, G. *Chem. Commun.* **2011**, *47*, 743. (c) Chu, J. X.; Lu, E. L.; Liu, Z.; Chen, Y.; Leng, X.; Song, H. *Angew. Chem., Int. Ed.* **2011**, *50*, 7677. (d) Jian, Z.; Rong, W.; Mou, Z.; Pan, Y.; Xie, H.; Cui, D. *Chem. Commun.* **2012**, *48*, 7516.

(16) (a) Knight, L. K.; Piers, W. E.; McDonald, R. *Organometallics* **2006**, *25*, 3289. (b) Knight, L. K.; Piers, W. E.; Fleurat-Lessard, P.; Parvez, M.; McDonald, R. *Organometallics* **2004**, *23*, 2087.

(17) (a) Shannon, R. D. *Acta Crystallogr.* **1976**, *A32*, 751. (b) Pauling, L. *The Nature of the Chemical Bond*, 3rd ed.; Cornell University Press: Ithaca, NY, 1960.

(18) (a) Andino, J. G.; Kilgore, U. J.; Pink, M.; Ozarowski, A.; Kyzstek, J.; Telsler, J.; Baik, M.-H.; Mendiola, D. J. *Chem. Sci.* **2010**, *1*, 351. (b) Basuli, F.; Kilgore, U. J.; Hu, X.; Meyer, K.; Pink, M.; Huffman, J. C.; Mendiola, D. J. *Angew. Chem., Int. Ed.* **2004**, *43*, 3156.

(19) (a) Flores, J. A.; Cavaliere, V. N.; Buck, D.; Pinter, B.; Chen, G.; Crestani, M. G.; Baik, M.-H.; Mendiola, D. J. *Chem. Sci.* **2011**, *2*, 1457. (b) Cavaliere, V. N.; Crestani, M. G.; Pinter, B.; Pink, M.; Chen, C.-H.; Baik, M.-H.; Mendiola, D. J. *J. Am. Chem. Soc.* **2011**, *133*, 10700. (c) Fout, A. R.; Scott, J.; Miller, D. L.; Bailey, B. C.; Pink, M.; Mendiola, D. J. *Organometallics* **2009**, *28*, 331. (d) Bailey, B. C.; Fan, H.; Huffman, J. C.; Baik, M.-H.; Mendiola, D. J. *J. Am. Chem. Soc.* **2007**, *129*, 8781. (e) Bailey, B. C.; Huffman, J. C.; Mendiola, D. J. *J. Am. Chem. Soc.* **2007**, *129*, 5302. (f) Bailey, B. C.; Fan, H.; Baum, E. W.;

Huffman, J. C.; Baik, M.-H.; Mindiola, D. J. *J. Am. Chem. Soc.* **2005**, *127*, 16016.

(20) For a general description of the equipment and techniques used in carrying out this chemistry, see: Burger, B. J.; Bercaw, J. E. *ACS Symp. Ser.* **1987**, *357*, 79.

(21) Pangborn, A. B.; Giardello, M. A.; Grubbs, R. H.; Rosen, R. K.; Timmers, F. J. *Organometallics* **1996**, *15*, 1518.

(22) See the Supporting Information.

(23) Masuda, J. D.; Wei, P.; Stephan, D. W. *Dalton Trans.* **2003**, 3500.

(24) APEX2; Bruker Analytical X-Ray Systems: Madison, WI, 2009.

(25) Blessing, R. *Acta Crystallogr.* **1995**, *A51*, 33.

(26) (a) Fan, L.; Foxman, B. M.; Ozerov, O. V. *Organometallics* **2004**, *23*, 326. (b) Fan, L.; Yang, L.; Guo, C.; Foxman, B. M.; Ozerov, O. V. *Organometallics* **2004**, *23*, 4778. (c) Ozerov, O. V.; Guo, C.; Papkov, V. A.; Foxman, B. M. *J. Am. Chem. Soc.* **2004**, *126*, 4792.

(27) Fryzuk, M. D.; Giesbrecht, G.; Rettig, S. J. *Organometallics* **1996**, *15*, 3329.

(28) Bailey, B. C.; Fout, A. R.; Fan, H.; Tomaszewski, J.; Huffman, J. C.; Mindiola, D. J. *Angew. Chem., Int. Ed.* **2007**, *46*, 8246.

(29) (a) Thompson, M. E.; Baxter, S. M.; Bulls, A. R.; Burger, B. J.; Nolan, M. C.; Santasiero, B. D.; Schaefer, W. P.; Bercaw, J. E. *J. Am. Chem. Soc.* **1987**, *109*, 203. (b) Shapiro, P. J.; Bunel, E.; Schaefer, W. P.; Bercaw, J. E. *Organometallics* **1990**, *9*, 867. (c) Watson, P. L.; Parshall, G. W. *Acc. Chem. Res.* **1985**, *18*, 51. (d) Watson, P. L. *J. Chem. Soc., Chem. Commun.* **1983**, 276. (e) Watson, P. L. *J. Am. Chem. Soc.* **1983**, *105*, 6491. (f) Sadow, A. D.; Tilley, T. D. *J. Am. Chem. Soc.* **2005**, *127*, 643. (g) Sadow, A. D.; Tilley, T. D. *J. Am. Chem. Soc.* **2003**, *125*, 7971. (h) Barros, N.; Eisenstein, O.; Maron, L.; Tilley, T. D. *Organometallics* **2008**, *27*, 2252. (i) Sadow, A. D.; Tilley, T. D. *Angew. Chem., Int. Ed.* **2003**, *42*, 803. (j) Fendrick, C. M.; Marks, T. J. *J. Am. Chem. Soc.* **1984**, *106*, 2214. (k) Bruno, J. W.; Smith, G. M.; Marks, T. J.; Fair, C. K.; Schultz, A. J.; Williams, J. M. *J. Am. Chem. Soc.* **1986**, *108*, 40.

(30) For some examples of pyridine C–H activation by an early transition metal or rare-earth metal, see: (a) Bi, S.; Lin, Z.; Jordan, R. F. *Organometallics* **2004**, *23*, 4882. (b) Guram, A. S.; Jordan, R. F. *Organometallics* **1991**, *10*, 3470. (c) Jordan, R. F.; Guram, A. S. *Organometallics* **1990**, *9*, 2116. (d) Jordan, R. F.; Taylor, D. F.; Baenziger, N. C. *Organometallics* **1990**, *9*, 1546. (e) Deelman, B.-J.; Stevels, W. M.; Teuben, J. H.; Lakin, M. T.; Spek, A. L. *Organometallics* **1994**, *13*, 3881. (f) den Haan, K. H.; Wielstra, Y.; Teuben, J. H. *Organometallics* **1987**, *6*, 2053.

(31) (a) Bailey, B. C.; Fan, H.; Huffman, J. C.; Baik, M.-H.; Mindiola, D. J. *J. Am. Chem. Soc.* **2006**, *128*, 6798. (b) Parham, W. E.; Piccirilli, R. M. *J. Org. Chem.* **1977**, *42*, 257.

(32) For comparison, titanium pyridyl complexes have also been structurally characterized. See: Bolton, P. D.; Clot, E.; Adams, N.; Dubberley, S. R.; Cowley, A. R.; Mountford, P. *Organometallics* **2006**, *25*, 2806.

(33) Activation of the 2-picolene CH₃ group has been reported and a similar η^3 binding mode has been observed with a yttrium complex. See: Duchateau, R.; Brussee, E. A. C.; Meetsma, A.; Teuben, J. H. *Organometallics* **1997**, *16*, 5506.

(34) (a) Standfuss, S.; Abinet, E.; Spaniol, T. P.; Okuda, J. *Chem. Commun.* **2011**, *47*, 11441. (b) Yu, N.; Nishiura, M.; Li, X.; Xi, Z.; Hou, Z. *Chem.—Asian J.* **2008**, *3*, 1406.

(35) (a) Huang, W.; Khan, S. I.; Diaconescu, P. L. *J. Am. Chem. Soc.* **2011**, *133*, 10410. (b) Hayes, P. G.; Piers, W. E.; Parvez, M. *Chem.—Eur. J.* **2007**, *13*, 2632.

(36) (a) Pool, J. A.; Scott, B. L.; Kiplinger, J. L. *J. Am. Chem. Soc.* **2005**, *127*, 1338. (b) Deelman, B.-J.; Stevels, W. M.; Teuben, J. H.; Lakin, M. T.; Spek, A. L. *Organometallics* **1994**, *13*, 3881.

(37) *CRC Handbook of Chemistry and Physics*, 92nd ed.; CRC Press: Boca Raton, FL, 2011.